NONLINEAR BEHAVIORS ANALYSIS AND NONLINEAR CHARACTERISTICS DIAGNOSING OF MECHANICAL VIBRATION SYSTEMS

A Thesis

Submitted to the Faculty of Graduate Studies and Research in Partial Fulfillment of the Requirements for the Degree of

Master of Applied Science

In

Industrial Systems Engineering

University of Regina

By

Dandan Xia

Regina, Saskatchewan

February, 2016

UNIVERSITY OF REGINA

FACULTY OF GRADUATE STUDIES AND RESEARCH

SUPERVISORY AND EXAMINING COMMITTEE

Dandan Xia, candidate for the degree of Master of Applied Science in Industrial Systems Engineering**,** has presented a thesis titled, ***Nonlinear Behaviors Analysis and Nonlinear Characteristics Diagnosing of Mechanical Vibration Systems,*** in an oral examination held on January 12, 2016. The following committee members have found the thesis acceptable in form and content, and that the candidate demonstrated satisfactory knowledge of the subject material.

External Examiner:	Dr. Yang Zhao, Department of Mathematics & Statistics
Supervisor:	Dr. Liming Dai, Industrial Systems Engineering
Committee Member:	Dr. Mehran Mehrandezh, Industrial Systems Engineering
Committee Member:	Dr. Mohamed Ismail, Industrial Systems Engineering
Chair of Defense:	Dr. Yee-Chung Jin, Environmental Systems Engineering

ABSTRACT

Comprehensive understanding and effective diagnosis of nonlinear behaviors are important in dynamical analyses of mechanical systems and may provide crucial guidance to the design and control of mechanical systems. In this research, the nonlinear behavior and stability of an elastic suspended cable under combined parametric and external excitations are studied first. Such cable is commonly used in suspended bridges. The governing equations of the cable with geometric nonlinearity are developed with considerations of the first in-plane and out-of-plane mode vibrations. The solutions of the nonlinear system are derived as per the perturbation method of higher accuracy. The nonlinear stability of the cable system is investigated in the research with focus on the influence of different system parameters on the stability. Multiple solutions of the system are found existing, corresponding to a single frequency of external excitation. With application of the Periodicity-Ratio (P-R) method, the effects of different external excitations on the nonlinear vibrations of the cable are examined. With a periodic-nonperiodic-chaotic region diagram developed on the basis of the P-R method, the nonlinear behavior of the cable can be quantified and graphically identified corresponding to a large range of external excitation.

In addition, to diagnose nonlinear behavior more accurately and efficiently, a proposed method combining the P-R method and Lyapunov exponent method is established in this research. The Lyapunov exponent method is probably the most widely used method in diagnosing nonlinear behaviors of dynamic systems. However, in comparing with the P-R method, Lyapunov approach is rather tedious in diagnosing the nonlinear

characteristics of a dynamic system. And also, Lyapunov exponent method may yield incorrect results for many cases. On the other hand, the P-R method describes the periodicity of a nonlinear system with a single value index and reveals the fact that there are actually infinite types of nonlinear behaviors in between periodic and chaotic cases. However, with the P-R method, it is difficult to directly distinguish between chaotic and quasiperiodic responses of a nonlinear system. With combination of the two methods, as shown in the research, nonlinear behaviors can be diagnosed much more accurately and efficiently. To demonstrate the advantages of the method proposed, the method combing the P-R and Lyapunov exponent methods is applied to analyze a dynamic system governed by Duffing's equation. Comparisons of the P-R and Lyapunov exponent methods are also conducted. The proposed method shows higher efficiency and reliability in comparing with either the Lyapunov exponent method or the P-R method.

ACKNOWLEDGEMENTS

The author would like to express her sincere appreciation to her supervisor, Dr. Liming Dai, for his patient guidance, expertise, and continuous support throughout the process of her Master of Applied Science program. The invaluable advice, encouragement, and financial support were important to the completion of this research.

The author also wishes to acknowledge Natural Sciences and Engineering Research Council of Canada (NSERC) for the financial support provided for the research, and the financial support from the Faculty of Graduate Studies and Research of the University of Regina in the form of Graduate Scholarships.

The author is highly appreciative of the advice from the committee members and would like to thank all her colleagues in the research group.

DEDICATION

Special thanks to my dear parents and brother for their continuous encouragement and unconditional support.

TABLE OF CONTENTS

TABLE OF FIGURES

LIST OF TABLES

CHAPTER1 INTRODUCTION

1.1 Background

For many years the analysis of the nonlinear behavior of mechanical vibrational systems has attracted substantial research effort. Systems that can be modeled by nonlinear algebraic or nonlinear differential equations are called nonlinear systems. Examples that appear frequently in mechanical vibrational systems such as pendulum, string, beam or cable. In 1899, Poincare studied nonlinear dynamics in the context of the *n* body problem in celestial mechanics. Based on the developed perturbation method, a geometrically inspired qualitative point of view, called a Poincare map was presented, which has been an essential criterion for nonlinear behavior. The study of nonlinear behavior made an important breakthrough when Cartwright and Littlewood (1945) observed chaos during their study on forced oscillations of the van der Pol oscillator. Lorenz (1963) studied a simple model of convection and observed a strange attractor through numerical simulation. Smale (1967) introduced the horseshoe map as an abstract prototype to explain chaotic motions. Poincare also noticed that the small differences in initial conditions may cause great changes in the final phenomena which is known to be a characteristic of system that exhibit chaotic behavior. Ruelle and Takens (1971) proposed a new theory for the onset of turbulence in fluids based on the abstract considerations about strange attractors. Feigenbaum (1970s) discovered universal laws governing the transition from regular motion to chaos. The nonlinear behavior, which has become very popular now, rejuvenated interest in nonlinear dynamics. Many important contributions which have been made through analytical, experimental, and numerical studies have been

documented through books such as Collet and Eckmann (1980), Mees (1981), Rasband (1990), and Ueda (1992).

The nonlinear behavior can also be seen in engineering application. An engineering structure such as a cable is widely used because of its flexibility, light damping and lightness. However, it is also because of these features that nonlinear characteristic cannot be neglected when studying its vibration. The nonlinear behavior such as chaos may cause heavy losses in engineering application, therefore, many studies have been conducted on the vibration of cables. The presence of internal resonances among different modes was obtained by Nayfeh (2000). The main feature of the vibrational system was first studied with numerical and geometrical techniques by Wiggins (1990). Meirovitch investigated the undamped nonlinear steady state solution of in-plane response of a taut-flat cable with a solution to Duffing's equation (1975). Perkins (1992) studied the nonlinear response of model interactions under parametric and external excitation. A three-dimensional case was studied by Takahashi and Konishi (1987) and nonlinear forced response was obtained. Global bifurcations and chaos were obtained in study of cable dynamics. Malhotra and Sri Namachchivaya (2002) applied the energy phase method and Galerkin's method to study the multi-pulse homoclinic orbits and chaotic dynamics. Zhang and Tang (1992) studied the global bifurcation and chaotic dynamics of a suspended elastic cable to small tangential vibration of one support based on the modified Melnikov method.

1.2 Research subjects and contributions

Nonlinear vibrations of cables have been studied for decades, the suspended cables subjected to parametric and external excitations are widely studied for their nonlinear characteristics. However, very few studies are found in the literature for the stability of cables, especially a suspended cable system. In the present research, a suspended cable system subjected to parametric and external excitations with a vibrating support at one end and a fixed support at the other is studied. This study intends to reveal the nonlinear behavior and stability of the cable system with higher accuracy and reliability in comparison with existing research found in the literature. Nonlinear behavioral investigations for suspended cables mainly focus on systems of unique system parameters and operation conditions. However, relatively large ranges of parameters and excitations are usually demanded in engineering design of nonlinear cables in the real world. With the implementation of a newly developed Periodicity-Ratio (P-R) method, this research reveals the nonlinear behavior of the suspended cable with a large range of system parameters. The results of this research may provide guidance for designing and analyzing nonlinear suspended cables used in various engineering fields.

In the study of the cable vibrations, a periodic-nonperiodic region diagram is presented to demonstrate the vibrational motion of the system. However, the quasi-periodic and chaotic cases cannot be distinguished by the P-R method. The P-R method and Lyapunov method are applied to diagnose the periodic, irregular quasi-periodic and chaotic cases. The Lyapunov exponent method has been widely used to diagnose chaos in nonlinear vibration investigations. The Periodicity-Ratio (P-R) method was first introduced by Dai and Singh in their study of nonlinear dynamical systems to describe the periodicity of a

nonlinear system. They can diagnose nonlinear behaviors and have advantages and disadvantages. Comparisons are conducted to show the advantages and disadvantages of the two methods. Combining the two methods, a region diagram is given to show all the nonlinear behaviors of the system.

CHAPTER 2 LITERATURE REVIEW

2.1 Nonlinear vibration

Nonlinear behavior exists in all fields including engineering, ecology and physics (Rinaldi and Muratori, 1993; Rinaldi et al., 1993; Gakkhar and Naji, 2003a) and so on. Nonlinear behavior in a vibrational system such as chaos may cause large amplitudes or instability in a system, therefore, the investigation of nonlinear vibrations is of great importance. Famous research was performed by Georg Duffing (1918) who studied the Duffing's equation. Duffing tackled the problem of a nonlinear oscillator in a systematic way. The nonlinear equation was described with a cubic nonlinearity. Since then, a lot of work have been done on this equation including the development of methods (both analytical and numerical) used to investigate the dynamic behavior of physical systems described by various forms of the Duffing's equation (Kovacic, 2011). By investigation of the Duffing's equation, an enormous range of well-known behaviors in nonlinear dynamic systems were exhibited such as chaos and quasiperiodic motion. Prior to Georg Duffing, researchers such as Poincare and Lyapunov also did a lot of research on nonlinear vibrations. As proposed by Poincare, the Poincare map have been widely used to study the nonlinear behavior of a vibrating system. The Lyapunov exponent, which is named after Lyapunov, is an important criterion for diagnosing chaos.

In the analysis of engineering systems, nonlinear behavior can always be found in structural vibrations. It is of particular importance in the study of nonlinearity in dynamics and vibration, because almost all applied processes act nonlinearly (Gladwell 2014). It is significant to understand nonlinear vibrations theoretically and numerically.

Nonlinear behavior is always caused by the geometric, material or excitation nonlinearities. Among these, geometric nonlinearity has been widely studied in vibrational analysis of structures in engineering applications. By their nature, the structures are typically made of highly flexible continuous elements such as beams, cables, strings and plates. It is also because of the flexibility of the structures that nonlinear analyses of complex systems is one the most important and complicated tasks, especially in engineering and applied science problems. However, nonlinear vibrations may cause behaviors such as chaos which result in large amplitudes or instability of structures. A lot of studies should be conducted on the investigation of nonlinear behavior. During the investigation of nonlinear systems, numerous methods were proposed for analysis such as D'Alembert's principle, the Newton method and Lagrange method (Rao, 1995). To solve the nonlinear problem, a numerical method was also presented by researchers such as the perturbation method, energy method, limit cycles, the differential transformation method and so on.

2.2 Nonlinear behavior of cables in Engineering

Cable is a very efficient structure in the application of engineering because of its flexibility, light weight, and light damping. The nonlinearity, such as geometric nonlinearity cannot be neglected. Early work on the dynamics of cables was conducted by d'Alembert, Euler, Bernoulli and Lagrange in the early eighteenth century. Hagedorn and Shafer (1980) discussed nonlinear free oscillations of suspended cables in case of small sag. They derived the original equation and discussed the nonlinear effect of the motions but only for the planar vibration. Luongo (1982) and his coworkers derived a simple mechanical model to analyze the in-plane and out-of-plane vibrations. In 1984,

Rega studied the large amplitude free vibration of a suspended cable with parametric excitations. Suitable equations for the system were obtained for large amplitude free vibrations. The main effect on frequency and temporal law of amplitude were studied for planar symmetric and anti-symmetric vibrational modes. The study of modal interactions of a suspended cable subjected to harmonic excitations at primary resonances has also been conducted in past decades. Perkins (1992), Benedettini (1995), Pakdemirli (1995) and Rega (1999) studied the nonlinear vibration of a cable by modeling the cable in different ways. Perkins studied the modal interactions of an elastic cable under parametric and external excitations. Benedettini derived a four-degree-of -freedom model of a suspended cable to study its nonlinear vibrations under multiple internal resonance conditions. Rega studied the primary resonance of the first in-plane symmetric mode with one-to-one internal resonance with two methods: The direct method and mode-reduce method. Frequency-response curves were obtained and show different qualitative and quantitative predictions for some nonlinear motions of the cable.

Other excitations such as random, wind, and fluid excitations were also studied by researchers with the development of studies on cables in engineering. Chang et al. (1996) investigated the nonlinear vibrations of an elastic cable under random excitations. The stochastic bifurcation of the out-of-plane mode is predicted by Gaussian and non-Gaussian closures. Numerical results show the non-Gaussian procedure can only predict bounded solutions within a limited region. The influence of statistics of the excitation level and cable parameters such as internal detuning, damping ratios and sag-to-span ratio were also studied. Martineli and Perotti (2001) numerically studied the nonlinear behavior under turbulent wind excitations. Taking geometrical and aerodynamic

nonlinearities into consideration, the dynamic behavior of a cable in 1:2 internal resonance conditions was studied.

Inclined cables which can be widely used in engineering, such as a cable-stayed bridge, also attracted researchers' interest. Zhao (2002), Nielsen and Kirkegaad (2002), Srinil (2003) studied the nonlinear dynamics of a cable-stayed bridge by deriving new models for the system and analysis by the perturbation method. The stability and influence of different coefficients were studied. In addition, a cable-beam structure was also studied by researchers because it can be closely modeled as in engineering application. Investigational results show the interaction between cable and beam can significantly affect the nonlinear behavior of the cable.

The stability and nonlinear characteristics of a suspended cable with fix-free boundary conditions, subjected to parametric and external excitations, is studied in the present research. The influence on nonlinear responses is discussed in the following chapters.

2.3 Diagnosing nonlinear behavior in Engineering

During the study of the nonlinear characteristics of a system, it is crucial to apply an efficient method to diagnose the periodic or chaotic motions of the system. The evidence for determining chaos came from a variety of experiments (Swiney 1984, Roux 1983, Brandstater 1983, Malaraison 1983, Guckenheimer 1983, Gollub 1980). Numerical methods were mentioned by Moon (1987) in the past decade to distinguish the chaotic motion from regular motion. Moon and his co-workers (1980) conducted experiments on buckled beams to show nonperiodic and chaotic behavior for forced excitations. Chaotic motion was shown using a Poincare map in the phase plane and strong attractors were

also distinguished by the Poincare projections and the phase angle of the forcing function. The curve representing three times the force amplitude was used as an experimental criterion for chaotic vibrations. Ciliberto and Gollub (1985) obtained a chaotic diagram in their experimental study of harmonically driven surface waves in a fluid cylinder. The distinguished chaotic and periodic motions for the wave were presented in the diagrams. There are also some criteria for chaos developed on the bases of the Lyapunov exponent and fractal dimension. Wolf (1984) first presented algorithms which allow the estimation of a non-negative Lyapunov exponent from an experimental time series. They monitored the long-term growth rate of small volume elements in an attractor. Experiments on the Belousov-Zhabotinskii reaction and Couette-Taylor flow were conducted to test the efficiency of the method. Doyne (1983) gave the definition of a dimension which can be easily computed. Dai and Singh (1997) proposed a method called the Periodicity-Ratio method to diagnose nonlinear motion by studying Duffing's equation. It describes the periodicity of the system by calculating the ratio of the overlapping points to the total points in a Poincare map. Dai and Han (2011) analyzed the periodicity, nonlinearity and transitional characteristics of a nonlinear system by the Periodicity-Ratio method. A multiple-periodicity diagram was generated so the periodicity and nonlinearity of the systems with respect to the system parameters can be graphed. The stability and convergence of the systems were investigated. Dai and Han (2011) also developed the Periodicity-Ratio method by comparing the overlapping conditions and characterizing the nonlinear dynamic system with a statistical hypothesis. The proposed Periodicity-Ratio is applied in the study of a nonlinear system in an engineering application (Dai and Wang 2013, Dai and Huang 2014, Zhang and Huang 2014).

CHAPTER 3 NONLINEAR RESPONSE AND STABILITY OF AN ELASTIC SUSPENDED CABLE SUBJECTED TO PARAMETRICAL EXTERNAL EXCITATIONS

3.1 Introduction

Cable structure is a very efficient structure in the engineering applications. Suspended cables are widely used in engineering structures such as bridges. In the past decades, nonlinear behavior of such cables has attracted great attention from numerous researchers and engineers. Among the research works in the literature, the studies on the suspended elastic cables are commonly seen in the field. Perkins (1992) derived a theoretical model to describe the nonlinear response of an elastic suspended cable. First order perturbation method was applied to study the stability and experimental results were compared to verify the accuracy of the research. Luongo (1982) in and his coworkers studied the planar nonlinear free vibration of an elastic suspended cable. They discussed the suitable values of cable properties to account for the nonlinear kinematical relations of the cable. Zhao (2002) analyzed the nonlinear behavior of an elastic cable subjected to a harmonic excitation using Garlerkin's method and method multiple scales. The coupled dynamic features between the in-plane and the out-of-plane vibration were analyzed. Arafat and Nayfeh (2002) study the nonlinear response of suspended cable with respect to primary resonance excitations. They applied the multi scales method directly to the nonlinear integral partial differential equations of the system for studying influence of the retained terms. Benedettini (1984) derived a four-degree-of-freedom model of a suspended cable

and possible steady state solutions such as unimodal and multimodal solution were studied and linearized stability was performed. Taking the geometric nonlinearity and the assumption of quasi-static into consideration, Wang and Zhao (2002) studied the nonlinear characteristics under three-to-one internal resonance.

The nonlinear characteristics of inclined cables also attracted attentions from the researchers in the field. Chen (2009) studied the bifurcations and chaos of an inclined cable. Averaging method was applied to study the primary resonance and 1:1 internal resonance. Global dynamics of the cable was also investigated and chaotic motion was found by numerical simulation results. Perturbation method was also applied to analysis the stability of the system and analysis of the system parameters based on a periodic solution.

Cable-beam coupled models are seen in investigating various types of cables in the real world particularly in studying nonlinear behavior of bridge structures. Gattulli (2003) and his co-workers proposed an analytical model to study the nonlinear interactions between beam and cable by a 2D discrete model. In the one-to-two global-local and two-to-one global-local resonance, a novel mechanism was analyzed and the well-known parametric-induced cable oscillation in stayed-systems is correctly reinterpreted. And in 2005, they also studied and verified the results by experimental and finite element methods. Fujino (1995) and co-authors investigated the auto-parametric resonance in a 3DOF model of cable-stayed-beam with experimental and analytical methods. In their research, a 3DOF analytical model of the structure was derived, where the finite motion of the cable introduced geometric nonlinearities in quadratic and cubic forms. In 2006, Xia studied the auto-parametric vibration of a cable-stayed-beam structure under random excitation.

Results show that when the vertical random excitation to the beam exceeds a critical value, the horizontal motions of the cable and beam are excited due to the auto-parametric nonlinear coupling. Similarly, such analysis can also be applied on the investigation of coupled string-beam system. As found in the literature, however, stabilities of the cables are not studies with the cable-beam models.

As discussed above, nonlinear vibration of cables is an interesting area of research for cables dynamics especially that of the cables used in bridges. The suspended cables subjected to parametric and external excitations are widely studies for their nonlinear characteristics. However, very few studies are found in the literature for the stability of the cables especially the suspended cable system considered in this research. In the present research, a suspended cable system subjected to parametric and external excitations with a vibrating support at one end and a fixed support at the other end is to be studied. This study intends to reveal the nonlinear behavior and stability of the cable system with an approach of higher accuracy and reliability in comparing with the existing research works found in the literature. One may also notice from the previous research works in this area that the nonlinear behavior investigations for the suspended cables mainly focused on the systems of unique system parameters and operation conditions. In engineering design of the nonlinear cables in the real world, however, relatively large ranges of parameters and excitations are usually demanded. With the implementation of a newly developed Periodicity-Ratio (P-R) method, this research is to reveal the nonlinear behavior of the suspended cable with considerations of large ranges of system parameters. The results of this research may therefore provide a useful guidance for

designing and analyzing the nonlinear suspended cables used in various engineering fields.

3.2 Model and governing equations

Our attention is focused on the vibration of an elastic cable of length L between a fixed support and a vibrating support excited by the prescribed oscillations $F(t) = F\cos\Omega_0 t$ in the tangential direction of equilibrium cable as shown in Figure 3.1. In this research, the vibration of in-plane and out-of-plane mode is considered.

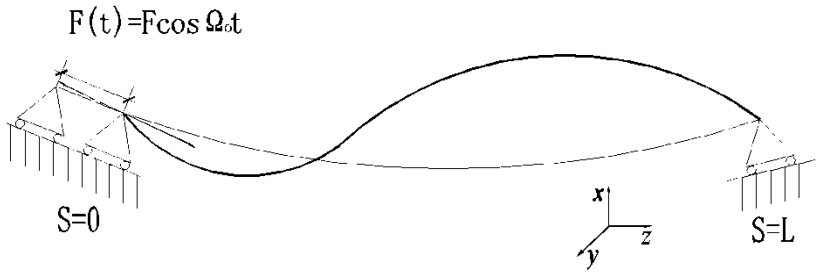

Figure 3.1 Model of the vibration system

The formulation of a two degree of freedom system can thus be given by the following governing equations of non-dimensional form:

$$\ddot{x} + 2\varepsilon^2 c_x\dot{x} + (\omega_x^2 + 2\varepsilon^2 f_1\cos\Omega t)x + \varepsilon^2\beta_3 xy^2 + \varepsilon^2\beta_4 x^3 - \varepsilon\alpha_2 y^2 - \varepsilon\alpha_3 x^2 = \varepsilon^2 F_1\cos\Omega t \tag{3.1}$$

$$\ddot{y} + 2\varepsilon^2 c_y\dot{y} + \left(\omega_y^2 + 2\varepsilon^2 f_2\cos\Omega t\right)y + \varepsilon^2\beta_1 y^3 + \varepsilon^2\beta_2 x^2 y - \varepsilon\alpha_1 xy = 0 \tag{3.2}$$

where x and y represent the displacement of in-plane and out-of-plane modes respectively with respect to time t, ω_x and ω_y indicate the natural frequencies of the

cable which are related to the geometric and material properties of the cable. c_x and c_y are the damping coefficients of the in-plane and out-of-plane modes. $\alpha_1, \alpha_2, \alpha_3, \beta_1, \beta_2,$ and β_3 are the nonlinear coefficients which are related to the properties of the cable and ε is a small dimensionless parameter, Ω is related to the amplitude of the excitation with the relationship $\Omega = \Omega_0\sqrt{\frac{L}{g}}$, and $f_1,$ and f_2 are related to the amplitude of the external excitations and the properties of the cable system. All the definitions and details of above coefficients can be found in Appendix A.

3.3 Solution development by Perturbation method

The multiple scale perturbation method is conducted to obtain a second-order approximation solution for Eqs. (3.1) and (3.2). With the assumption:

$$x(\varepsilon, t) = x_0(T_0, T_1, T_2) + \varepsilon x_1(T_0, T_1, T_2) + \varepsilon^2 x_2(T_0, T_1, T_2) \tag{3.3}$$

$$y(\varepsilon, t) = y_0(T_0, T_1, T_2) + \varepsilon y_1(T_0, T_1, T_2) + \varepsilon^2 y_2(T_0, T_1, T_2) \tag{3.4}$$

where $T_n = \varepsilon^n t$ $(n = 0,1,2 \ldots)$ are the fast and slow time scales respectively. The time derivations can be described as:

$$\frac{d}{dt} = \frac{\partial}{\partial T_0}\frac{\partial T_0}{\partial t} + \frac{\partial}{\partial T_1}\frac{T_1}{\partial t} + \cdots, = D_0 + \varepsilon D_1 + \cdots,$$

$$\frac{d^2}{dt^2} = D_0^2 + 2\varepsilon D_0 D_1 + \varepsilon^2(D_1^2 + 2D_0 D_2) \tag{3.5}$$

where $D_n = \frac{\partial}{\partial T_n}$,

In terms of stability of the cable system considered, the worst scenario is the vibration at resonance, which can be the resonances in both the in-plane and out-of-plane modes. In this research, the responses of the cable system of 1:1 internal resonance and ½ sub-harmonic resonance together with the responses at the vicinities of the two resonances are considered. As such, the following relationships are assumed.

$$\omega_x^2 = \frac{1}{4}\Omega^2 + \varepsilon^2\sigma_1, \quad \omega_y^2 = \frac{1}{4}\Omega^2 + \varepsilon^2\sigma_2, \tag{3.6}$$

Let $\omega = \frac{1}{2}\Omega$, substitute (3.5) and (3.6) into (3.3) and (3.4), and then equate the coefficients of same power of ε in both sides, one may obtain:

Order ε^0:

$$D_0^2 x_0 + \omega^2 x_0 = 0, \tag{3.7}$$

$$D_0^2 y_0 + \omega^2 y_0 = 0, \tag{3.8}$$

Order ε^1:

$$D_0^2 x_1 + \omega^2 x_1 = -2D_0 D_1 x_0 + \alpha_2 y_0^2 + \alpha_3 x_0^2, \tag{3.9}$$

$$D_0^2 y_1 + \omega^2 y_1 = -2D_0 D_1 x_1 + \alpha_1 x_0 y_0, \tag{3.10}$$

Order ε^2:

$$D_0^2 x_2 + \omega^2 x_2 = -2D_0 D_1 x_1 - (D_1^2 + 2D_0 D_2)x_0 - 2c_x D_0 x_0 - \sigma_1 x_0 2f_1 \cos(\Omega T_0)\, x_0 - \beta_3 x_0 y_0^2 - \beta_4 x_0^3 + 2\alpha_2 y_0 y_1 + 2\alpha_3 x_0 x_1 + F\cos(\Omega T_0), \tag{3.11}$$

$$D_0^2 y_2 + \omega^2 y_2 = -2D_0 D_1 y_1 - (D_1^2 + 2D_0 D_2)y_0 - 2c_y D_0 y_0 - 2f_2 \cos(\Omega T_0)\, y_0 -$$

$$\sigma_2 x_0 - \beta_1 y_0^3 - \beta_2 x_0^2 y_0 + \alpha_1 (x_0 y_1 + x_1 y_0),$$

(3.12)

The general solution of the partial differential equations Eqs. (3.7)-(3.8) can be expressed as:

$$x_0 = A_1(T_1, T_2) e^{i\omega T_0} + cc \tag{3.13}$$

$$y_0 = A_2(T_1, T_2) e^{i\omega T_0} + cc \tag{3.14}$$

where A_1 and A_2 are complex functions in T_1 and T_2 and *cc* is the corresponding complex conjugate term. Substituting Eqs. (3.13)-(3.14) into Eqs. (3.9)-(3.10) and eliminating the secular terms, the bounded first-order approximation yields:

$$x_1 = \frac{\alpha_2 A_2 \overline{A_2} + \alpha_3 A_1 \overline{A_1}}{\omega^2} - \frac{\alpha_2 A_2^2 + \alpha_3 A_1^2}{3\omega^2} e^{2i\omega T_0} + cc$$

$$y_1 = \frac{\alpha_1 A_1 \overline{A_2}}{\omega^2} - \frac{\alpha_1 A_1 A_2}{3\omega^2} e^{2i\omega T_0} + cc$$

(3.15)

From the elimination of the secular terms, we have $D_1 A_1 = 0, D_1 A_2 = 0$ which indicates that A_1 and A_2 are the functions with respected to T_2 only. Substituting Eqs. (3.13), (3.14) and (3.15) into Eqs. (3.11) and (3.12), one may obtain

$$
\begin{aligned}
D_0^2 x_2 + \omega^2 x_2 = & -2i\omega D_1 A_2 e^{i\omega T_0} - 2i\omega c_x A_1 e^{i\omega T_0} - \sigma_1 A_1 e^{i\omega T_0} - 2f_1 \cos(\Omega T_0) A_1 e^{i\omega T_0} \\
& - \left[\beta_3 A_1 A_2^2 e^{3i\omega T_0} + (2\beta_3 A_1 A_2 \overline{A_2} + \beta_3 \overline{A_1} A_2^2) e^{i\omega T_0}\right] - \beta_4 A_1^3 e^{3i\omega T_0} \\
& - 3\beta_4 A_1^2 \overline{A_1} e^{i\omega T_0} + \frac{2\alpha_1\alpha_2 A_1 A_2 \overline{A_2} + 2\alpha_1\alpha_2 \overline{A_1} A_2^2}{\omega^2} e^{i\omega T_0} \\
& - \frac{2\alpha_1\alpha_2 A_1 A_2 \overline{A_2}}{3\omega^2} e^{i\omega T_0} - \frac{2\alpha_1\alpha_2 A_1 A_2^2}{3\omega^2} e^{3i\omega T_0} \\
& + \frac{4\alpha_2\alpha_3 A_1 A_2 \overline{A_2} + 4\alpha_3^2 \overline{A_1} A_1^2}{\omega^2} e^{i\omega T_0} - \frac{2\alpha_2\alpha_3 \overline{A_1} A_2^2 + 2\alpha_3^2 \overline{A_1} A_1^2}{3\omega^2} e^{i\omega T_0} \\
& - \frac{2\alpha_2\alpha_3 A_1 A_2^2 + 2\alpha_3^2 A_1^3}{3\omega^2} e^{3i\omega T_0} + NST + cc
\end{aligned}
\tag{3.16}
$$

$$
\begin{aligned}
D_0^2 y_2 + \omega^2 y_2 = & -2i\omega D_2 A_2 e^{i\omega T_0} - 2i\omega c_y A_2 e^{i\omega T_0} - 2f_2 \cos(\Omega T_0) A_2 e^{i\omega T_0} \\
& - \beta_1 A_2^3 e^{3i\omega T_0} - 3\beta_1 A_2^2 \overline{A_2} e^{i\omega T_0} - \beta_2 A_1^2 A_2 e^{3i\omega T_0} - \beta_2 A_1^2 \overline{A_2} e^{i\omega T_0} \\
& - 2\beta_2 \overline{A_1} A_1 A_2 e^{i\omega T_0} + \frac{\alpha_1^2 A_1^2 \overline{A_2}}{\omega^2} e^{i\omega T_0} - \frac{\alpha_1^2 A_1^2 A_2}{3\omega^2} e^{3i\omega T_0} + \frac{\alpha_1^2 A_1 A_2 \overline{A_1}}{\omega^2} e^{i\omega T_0} \\
& - \frac{\alpha_1^2 A_1 A_2 \overline{A_1}}{3\omega^2} e^{i\omega T_0} + \frac{2\alpha_1\alpha_2 \overline{A_2} A_2^2 + 2\alpha_1\alpha_3 A_1 A_2 \overline{A_1}}{\omega^2} e^{i\omega T_0} \\
& - \frac{\alpha_1\alpha_2 A_2^3 + \alpha_1\alpha_3 A_1^2 A_2}{3\omega^2} e^{3i\omega T_0} - \frac{\alpha_1\alpha_2 A_2^2 \overline{A_2} + \alpha_1\alpha_3 A_1^2 \overline{A_2}}{3\omega^2} e^{i\omega T_0} + NST \\
& + cc
\end{aligned}
\tag{3.17}
$$

where NST and cc represent the non-secular and the complex conjugate terms respectively.

Eliminating the secular terms from Eqs. (3.16) and (3.17), one may obtain:

$$2i\omega D_2 A_1 = -2i\omega c_x A_1 - \sigma_1 A_1 - f_1\overline{A_1} + \gamma_1 A_1 A_2\overline{A_2} + \gamma_2 A_1^2\overline{A_1} + \gamma_3\overline{A_1}A_2^2 \quad (3.18)$$

$$2i\omega D_2 A_2 = -2i\omega c_y A_2 - \sigma_2 A_2 - f_2\overline{A_2} + \gamma_4 A_2^2\overline{A_2} + \gamma_5 A_1^2\overline{A_2} + \gamma_6\overline{A_1}A_1 A_2 \quad (3.19)$$

The expressions for $\gamma_1, \gamma_2, \gamma_3, \gamma_4, \gamma_5, \gamma_6$ can be seen in the Appendix B.

Introducing the polar form notations $A_1 = ae^{i\theta_1}$; and $A_2 = be^{i\theta_2}$, where a, b are the steady-state amplitudes of the vibration and θ_1, θ_2 are the phases of the vibration respectively. Separating the real and imaginary parts in Eqs. (3.18) and (3.19),, the governing equations of amplitudes and phases can be given by:

$$a' = -c_x a + \frac{f_1}{2\omega} a \sin 2\theta_1 \quad (3.20)$$

$$a\theta_1' = \frac{\sigma_1}{2\omega} a + \frac{f_1}{2\omega} a \cos 2\theta_1 - \frac{1}{2\omega}(\gamma_1 ab^2 + \gamma_2 a^3) - \frac{\gamma_3}{2\omega} ab^2 \quad (3.21)$$

$$b' = -c_y b + \frac{f_2}{2\omega} b \sin 2\theta_2 \quad (3.22)$$

$$b\theta_2' = \frac{\sigma_2}{2\omega} b + \frac{f_2}{2\omega} b \cos 2\theta_2 - \frac{\gamma_4}{2\omega} b^3 - \frac{\gamma_5}{2\omega} a^2 b - \frac{\gamma_6}{2\omega} a^2 b \quad (3.23)$$

For the steady-state solutions, one may have to have the conditions of $a' = b' = \theta_1' = \theta_2' = 0$. When these conditions are satisfied, Eqs. (3.20)-(3.23) can be rewritten as:

$$-c_x a + \frac{f_1}{2\omega} a \sin 2\theta_1 = 0 \quad (3.24)$$

$$\frac{\sigma_1}{2\omega} + \frac{f_1}{2\omega}\cos 2\theta_1 - \frac{1}{2\omega}(\gamma_1 b^2 + \gamma_2 a^2) - \frac{\gamma_3}{2\omega} b^2 = 0 \quad (3.25)$$

$$-c_y b + \frac{f_2}{2\omega} b \sin 2\theta_2 = 0 \quad (3.26)$$

$$\frac{\sigma_2}{2\omega} + \frac{f_2}{2\omega}\cos 2\theta_2 - \frac{\gamma_4}{2\omega} b^2 - \frac{\gamma_5}{2\omega} a^2 - \frac{\gamma_6}{2\omega} a^2 = 0 \quad (3.27)$$

Solutions of Eqs. (3.24)-(3.27) can be classified into single-mode solution and two mode solution as shown in the following cases.

Case 1: $a = 0; b \neq 0$. Squaring (3.26) an (3.27) and adding the results together then it can be written as:

$$\gamma_4^2 b^4 - 2\sigma_2\gamma_4 b^2 + \left(\sigma_2^2 + 4c_y^2\omega^2\right) - f_2^2 = 0 \tag{3.28}$$

Case 2: $b = 0; a \neq 0$. Squaring (24) an (25) and adding the results together then it can be written as:

$$\gamma_2^2 a^4 - 2\sigma_1\gamma_2 a^2 + (\sigma_1^2 + 4\omega^2 c_x^2 - f_1^2) \tag{3.29}$$

Case 3: $a \neq 0, b \neq 0$, squaring the equations similarly with case 1 and case 2, the following frequency response can be obtained:

$$\tau_1 a^4 + \tau_2 a^2 + \tau_3 = 0 \tag{3.30}$$

$$\tau_4 b^4 + \tau_5 b^2 + \tau_6 = 0 \tag{3.31}$$

where $\tau_1, \tau_2, \tau_3, \tau_4, \tau_5, \tau_6$ are expressed in Appendix C.

3.4 Stability analysis

3.4.1 Stability of the trivial solutions

For the sake of stability analysis, trivial solutions of the system are firstly considered. For this purpose, the governing equations Eqs. (3.18) and (3.19) are linearized. Introducing the following expresses $A_1 = x_1 + iy_1; A_2 = x_2 + iy_2$, where $x_{1,2}$ and $y_{1,2}$ are real functions with respect to T_2, and separating the real and imaginary parts, the governing equations Eqs. (3.18) and (3.19) can be rewritten as

$$x_1' = -c_x x_1 - \frac{\sigma_1}{2\omega} y_1 + \frac{f_1}{2\omega} y_1 \tag{3.32}$$

$$y_1' = -c_x y_1 + \frac{\sigma_1}{2\omega} x_1 + \frac{f_1}{2\omega} x_1 \tag{3.33}$$

$$x_2' = -c_y x_2 - \frac{\sigma_2}{2\omega} y_2 + \frac{f_2}{2\omega} y_2 \tag{3.34}$$

$$y_2' = -c_y y_2 + \frac{\sigma_2}{2\omega} x_2 + \frac{f_2}{2\omega} x_2 \tag{3.35}$$

The stability of a particular fixed point along the cable for the above autonomous ordinary differential equations is determined by the eigenvalues of the following equation:

$$\lambda^4 + k_1\lambda^3 + k_2\lambda^2 + k_3\lambda + k_4 = 0 \tag{3.36}$$

The eigenvalues of the equation is:

$$\lambda = -c_x \pm \frac{\sqrt{f_1^2 - \sigma_1^2}}{2\omega} \text{ and } \lambda = -c_y \pm \frac{\sqrt{f_2^2 - \sigma_2^2}}{2\omega}$$

The system is considered as stable if the eigenvalues have negative real parts, otherwise it is unstable. As we can see from the expression, the stable and unstable region is only related to the values of $f_1, f_2, c_x, c_y, \sigma_1, \sigma_2, \omega$. With the fixe values of these coefficients, if the eigenvalue λ have a negative real part, the system is stable, otherwise unstable.

3.4.2 Stability of the non-trivial solutions

To study the stability of the non-trivial solutions, the steady-state solutions can be linearize as:

$$a = a_0 + a_1, b = b_0 + b_1, \theta_1 = \theta_{10} + \theta_{11}, \theta_2 = \theta_{20} + \theta_{21} \tag{3.37}$$

where $a_0, b_0, \theta_{10}, \theta_{20}$ are the steady state values, and $a_1, b_1, \theta_{11}, \theta_{21}$ are the perturbation values, substituting them into Eq. (3.20)-(3.23) and keep the linear terms, one may obtain:

$$a_1' = \left(-c_x + \frac{f_1}{2\omega}\sin 2\theta_{10}\right) a_1 + \left(\frac{f_1}{\omega} a_0 \cos 2\theta_{10}\right) \theta_{11} \tag{3.38}$$

$$\theta_{11}' = \left(-\frac{f_1}{\omega}\sin 2\theta_{10}\right) \theta_{11} - \left(\frac{\gamma_1+\gamma_3}{\omega} b_0\right) b_1 - \left(\frac{\sigma_1}{2\omega} + \frac{f_1}{2\omega}\cos 2\theta_{10} - \frac{3\gamma_2}{2\omega} a_0^2 - \frac{\gamma_1+\gamma_3}{2\omega} b_0^2\right) \frac{a_1}{a_0} \tag{3.39}$$

$$b_1' = \left(-c_y + \frac{f_2}{2\omega}\sin 2\theta_{20}\right) b_1 + \left(\frac{f_1}{\omega} a_0 \cos 2\theta_{20}\right) \theta_{21} \tag{3.40}$$

$$\theta_{21}' = \left(-\frac{f_2}{\omega}\sin 2\theta_{20}\right) \theta_{21} - \left(\frac{\gamma_5+\gamma_6}{\omega} a_0\right) a_1 - \left(\frac{\sigma_2}{2\omega} + \frac{f_2}{2\omega}\cos 2\theta_{20} - \frac{3\gamma_4}{2\omega} b_0^2 - \frac{\gamma_5+\gamma_6}{2\omega} a_0^2\right) \frac{b_1}{b_0} \tag{3.41}$$

The necessary and sufficient condition of the system to be stable is determined by the real part of the Jacobian matrix of the right side of the Eqs. (3.38) - (3.41). The system is stable if the eigenvalues have negative real parts, otherwise the system is unstable.

3.5 Numerical simulation

With non-trivial solutions developed in the previous section, the stability analyses for the cable system considered are numerically conducted corresponding to the two mode solutions. In this research, MatLab 2013 is implemented for the numerical simulations. As mentioned previously, the worst scenario of the cable's vibratory responses is at the resonances of the system. The focus of the research is therefore at the resonances for both the in-plane and out-of-place modes. The numerical simulations are hence conducted for the responses of the cable system at the resonances and at the vicinities of the resonances. Various system parameters and external excitations are considered and the responses of

the cable system are plotted in frequency-response curves, to demonstrate the stabilities of the system. The detuning parameters σ_1 and σ_2 are the parameters controlling the frequencies at the vicinities of that of the resonances. The effects of detuning parameters on amplitudes are therefore studied specifically. Stability areas are determined and the effects of different parameters are investigated, corresponding to the detuning parameters.

3.5.1 Frequency-response curves of non-trivial solutions

For the non-trivial cases, Figure 3.2-3.9 show the frequency-response curves of the solutions for two mode where multi-values can be found from the geometry of the Figures. Figures 3.4 and 3.5 show the influence of ω on in-plane and out-of-plane mode respectively. As seen from the Figures, the vibration amplitude decreases and the two branches of solutions converge to each other as the decrease of the natural frequency. Figure3.6 and 3.7 show the influence of the different parameters, such as β_1, β_4, f_1 and f_2, on the frequency-response curves. Figure 3.6 illustrates the effect of β_4 on in-plane mode. With the increase of β_4, both the vibration amplitude and the region of unstable responses of the cable increase. The region of multi-value solutions is increased as well. Figure 3.7 exhibits the influence of β_1, which is a cubic term in the governing equation. As the β_1 increase, the vibration amplitude of out-of-plane mode increases significantly and the unstable region increases as well. Figures 3.8 and 3.9 show the influences of f_1 and f_2 which are related to the amplitude of the external excitation. From the Figures, it can be seen that amplitude of out-of-plane mode is proportional to f_1. As the increase of f_2, the amplitude of in-plane mode increase.

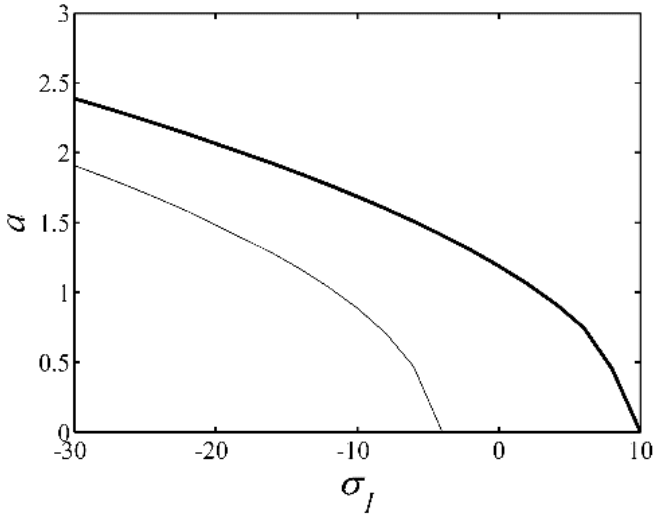

Figure 3.2: Frequency-response curves of the in-plane mode for basic case f_1=f_2=5.86 ω =4.28

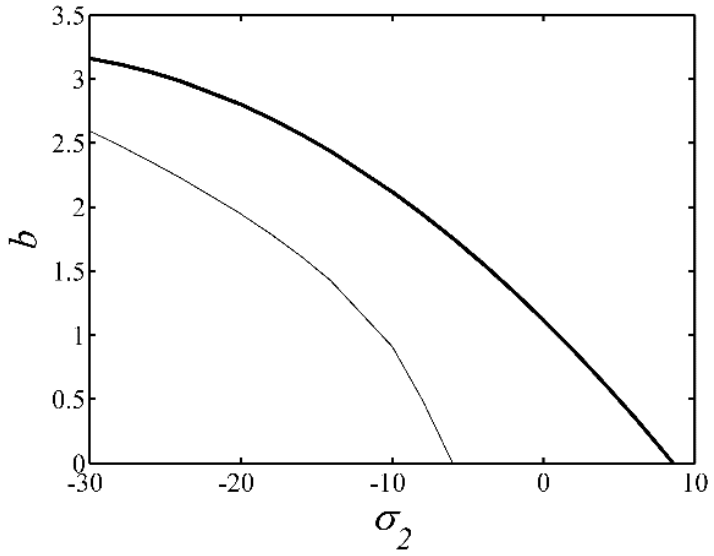

Figure 3.3: Frequency-response curves of the out-of-plane mode for basic case f_1=f_2=5.86 ω =2.38

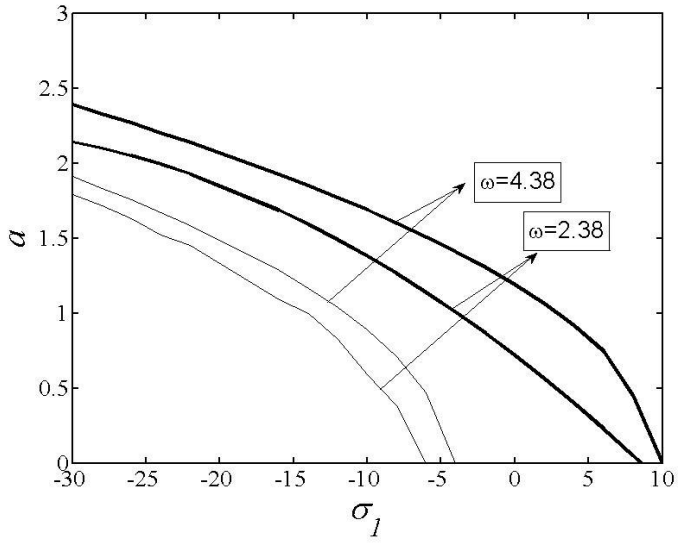

Figure 3.4: Frequency-response curves: influence of ω on in-plane mode

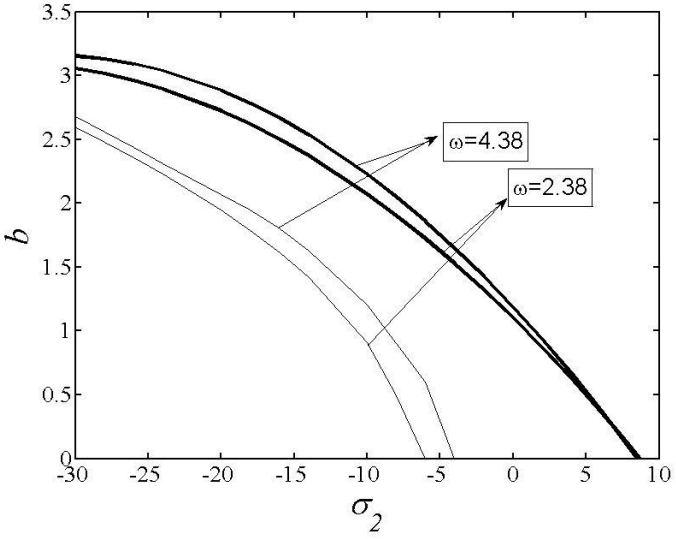

Figure 3.5: Frequency-response curves: influence of ω on out-of-plane mode

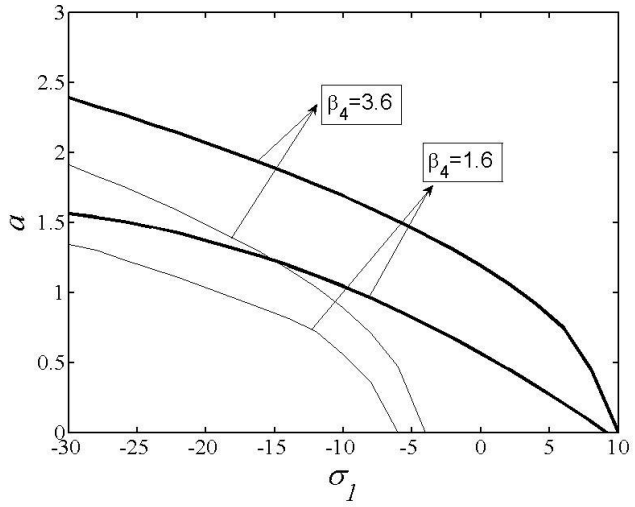

Figure 3.6: Frequency-response curves: influence of β_4 on in-plane mode

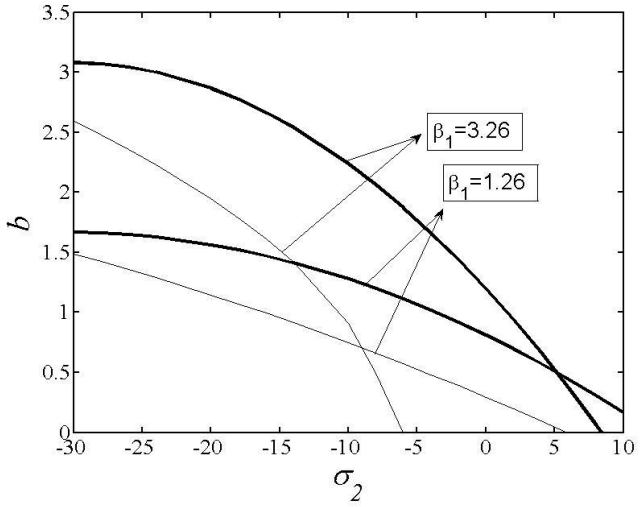

Figure 3.7: Frequency-response curves: influence of β_1 on out-of-plane mode

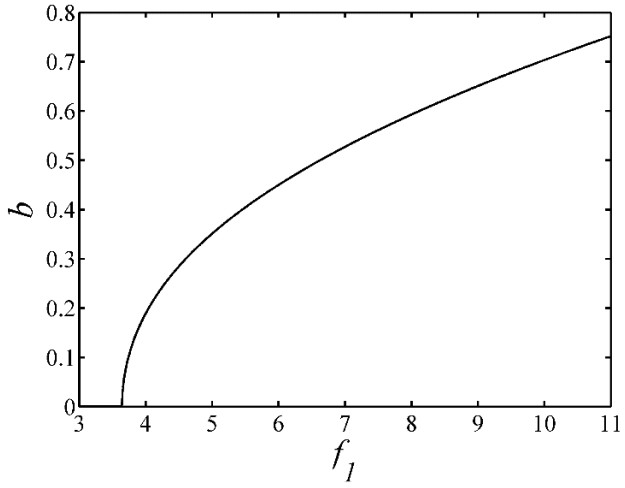

Figure 3.8: Frequency-response curves: influence of f_1 on out-of-plane mode

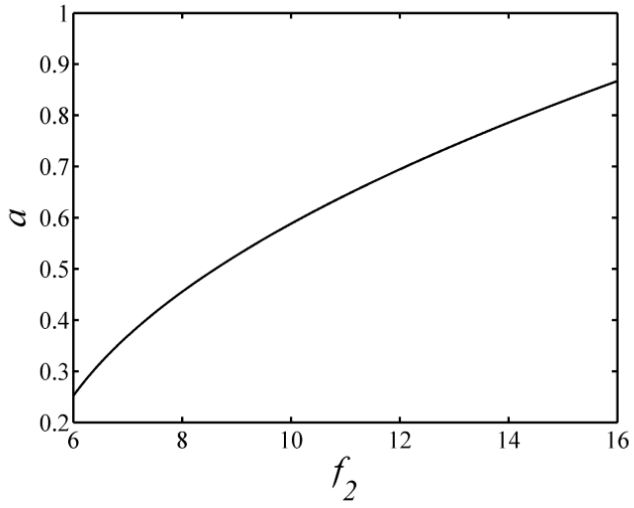

Figure 3.9: Frequency-response curves: influence of f_2 on in-plane mode

3.6 Analysis and characterization of the cable's nonlinear responses

The cable system considered in this research is nonlinear as expressed in the governing Eqs.(3.1) and (3.2). For such nonlinear cable system with the boundaries as shown in Figure 1, several authors reported their analyses for the nonlinear behavior of the cable. However, all the analyses were for a given system with unique system parameters and conditions. For engineering design practices, a range of system parameters is commonly demanded to be taken into consideration. In order to fulfill this requirement, in this research, a single value index, named the Periodicity-Ratio (P-R), is implemented.

3.6.1 The P-R method

The P-R method was first introduced by Dai and Singh in their study of nonlinear dynamic systems for diagnosing periodic, quasi-periodic and chaotic responses of the systems. The P-R method considers the geometry of Poincare maps. Based on Poincare map, the nonlinear dynamic behavior can be characterized by single value index, defined by the following expression.

$$\gamma = \lim_{n\to\infty} \frac{NOP}{n} \tag{3.42}$$

where NOP denotes the number of overlapping periodic points and n is the total number of points in the Poincare map, and NOP can be defined as:

$$NOP = \zeta(1) + \sum_{k=2}^{n} \zeta(\mathrm{k})\, P\left(\prod_{l=1}^{k-1}\{X_{kl} + \dot{X}_{kl}\}\right) \tag{3.43}$$

where $\zeta(\mathrm{k})$ indicates the number of points overlapping with the kth visible point in the Poincare map, and X_{kl}, $\dot{X}_{kl}$ and P can be defined as:

$$X_{kl} = |X(\tau_0 + kT) - X(\tau_0 + lT)|$$

$$\dot{X}_{kl} = \left|\dot{X}(\tau_0 + kT) - \dot{X}(\tau_0 + lT)\right|$$

$$\mathrm{P(Z)} = \begin{cases} 0 & if\ Z = 0 \\ 1 & if\ Z \neq 0 \end{cases} \tag{3.44}$$

As pointed out in the literature, the P-R value γ can be used as a criterion to characterize the nonlinear behaviors of a nonlinear dynamic system. If a system is periodic, all the points in the corresponding Poincare map are overlapping periodic points, i.e., the P-R value γ equals to one. The system will be quasi-periodic or chaotic if γ equals to 0. The P-R value is therefore an index quantifies the periodicity of a nonlinear dynamic system. Based on the P-R method, the nonlinear behavior such as periodicity, quasiperiodicity, chaos and other nonlinear behavior of a nonlinear system can be easily diagnosed.

3.6.2 Nonlinear behavior of the cable system diagnosed by the P-R values

The cable system considered and analyzed numerically with utilization of the fourth-order Runge-Kutta method. The responses of the cable system are complex. Various behaviors of the system are found and plotted in Figure 3.10 - Figure 3.24. Simulation results show the periodic, quasi-periodic and chaotic motions exist in the vibration of the system. With different P-R values, the different dynamic behavior can be found in under different system parameters which can check the accuracy of the method. Figure 3.10 and 3.12 show phase diagram of in-plane mode and out-of-plane respectively with P-R values equal to 1 and Ω =4.77, $F_1 = 30.1$. We set the values of coefficients $c_x = c_y = 0.32, \omega_x = \omega_y = 2.38$. From the Poincare map in Figure 3.11 and Figure 3.13we can see the periodic motion of the system which agree with P-R value. Figure 3.14 - Figure 3.21

show the phase diagram and Poincare map of in-plane and out-of-plane mode when P-R values equal to 0. We can conclude that both chaotic and quasi-periodic motions can be distinguished in this case. With a little change of Ω, the system can be shifted to periodic to non-periodic which indicates the sensitivity of the nonlinear system. However, with the P-R values in between 0 and 1, there are a lot of irregular motions as shown in Figure 3.22 - Figure 3.26 with P-R values equal to 0.47 and 0.26 in in-plane and out-of-plane mode respectively. The accuracy of P-R method can be verified in this section and it can be seen that there exists motions between periodic and non-periodic.

With the application of P-R method, the influence of parameters can be clearly distinguished. To study the influence of the amplitude and frequency of the excitation, a region-diagram of in-plane mode is plotted as shown in Figure 3.26.

In this section, nonlinear characteristics of the two-degree-of-freedom are studied. Simulation results show periodic and chaotic characters of the system. In the above study, we considered the stability of the parametric resonance and 1:1 internal resonance for the symmetric in-plane and out-of-plane modes with ½ sub-harmonic resonance for the in-plane mode. Therefore, to study the effect of the excitation on nonlinear behavior of the cable, a periodic-quasiperiodic-chaotic region diagram with excited frequency around twice of natural frequency of in-plane mode is given to diagnose the periodic and non-periodic motion of the system efficiently with application of P-R method.

In the region diagram, each of the point represents the different PR value corresponding to different values of variables. The blue points indicate the periodic motion with PR values equal to 1, the black points represent the irregular motion with PR value in between 0 and 1. However, the red points indicate the chaotic motion. We study the ½

sub-harmonic resonance case for the in-plane mode with $\omega_x = 2.38$, it can be seen from the region diagram, the dynamic behavior of the in-plane mode is related to both amplitude and frequency of the excitation. With a small excitation, the vibration is periodic near the $2\omega_x$. The chaotic motion can be easily found with large amplitude.

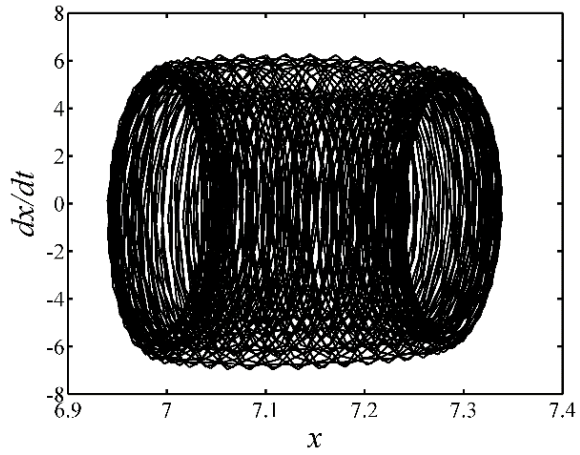

Figure 3.10: Phase diagram of in-plane mode with PR=1

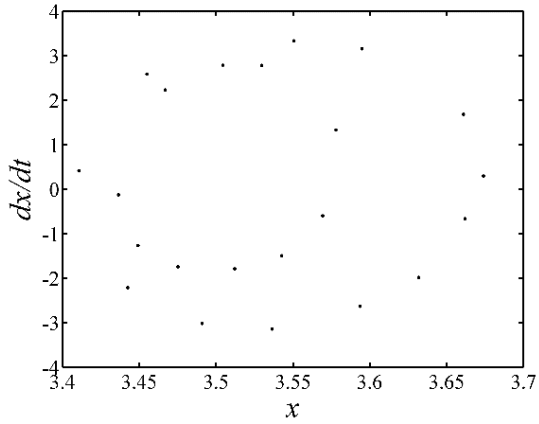

Figure 3.11: Poincare map of in-plane mode with PR=1

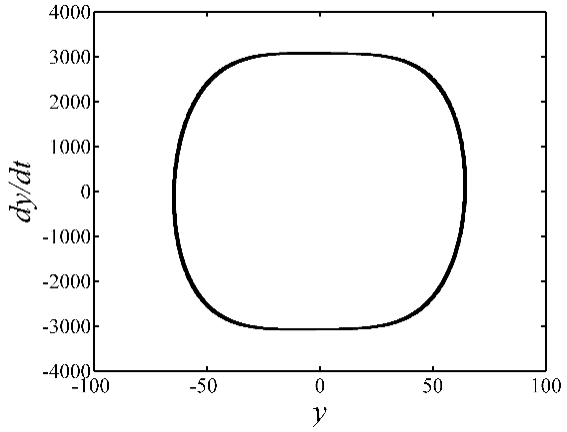

Figure 3.12: Phase diagram of out-of-plane mode with PR=1

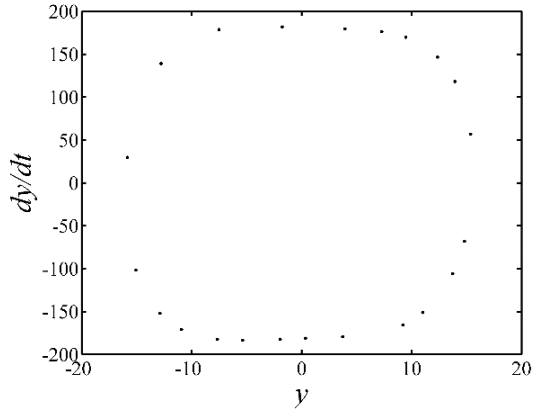

Figure 3.13: Poincare map of out-of-plane mode with PR=1

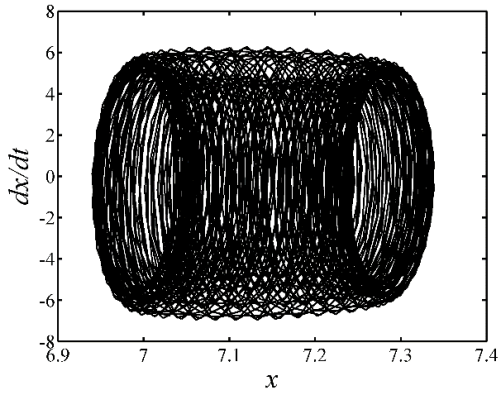

Figure 3.14: Phase diagram of in-plane mode with PR=0

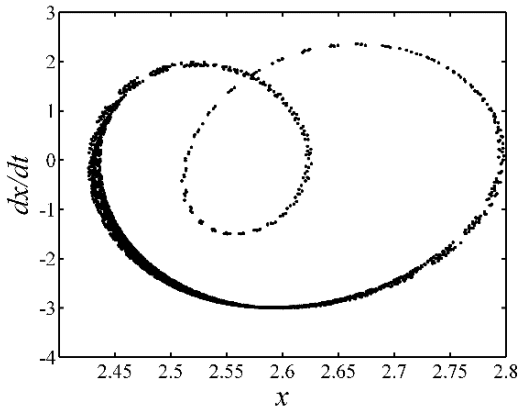

Figure 3.15: Poincare map of in-plane mode with PR=0

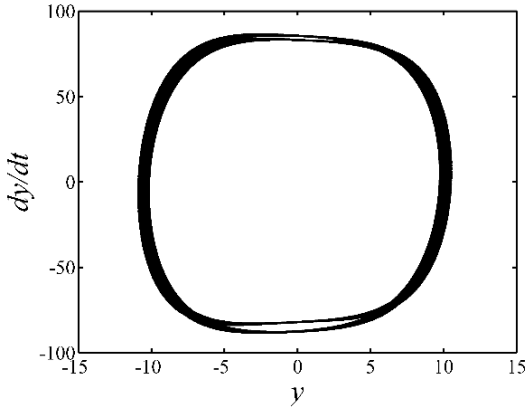

Figure 3.16: Phase diagram of out-of-plane mode with PR=0

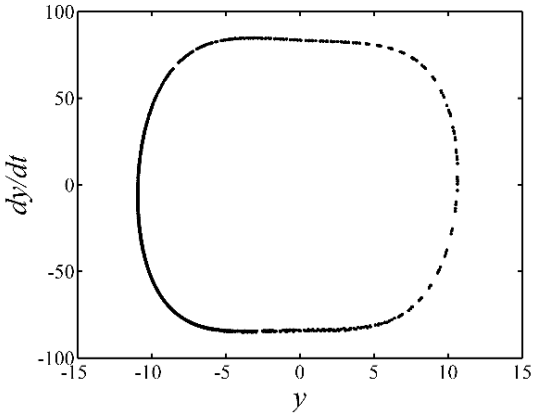

Figure 3.17: Poincare map of out-of-plane mode with PR=0

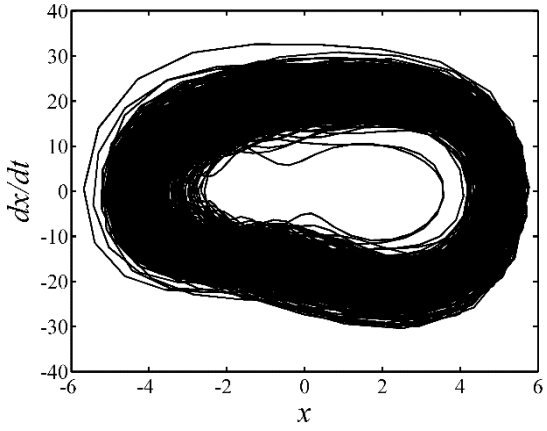

Figure 3.18: Phase diagram of in-plane mode with PR=0

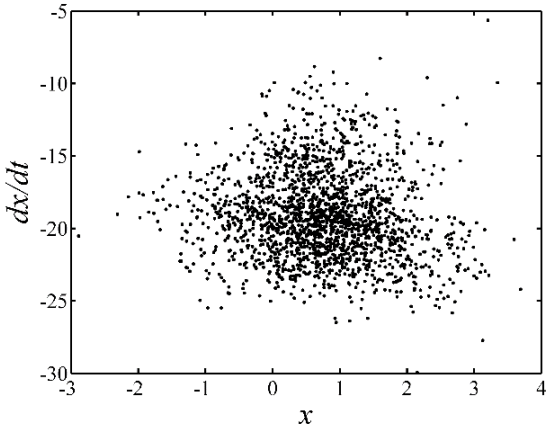

Figure 3.19: Poincare map of in-plane mode with PR=0

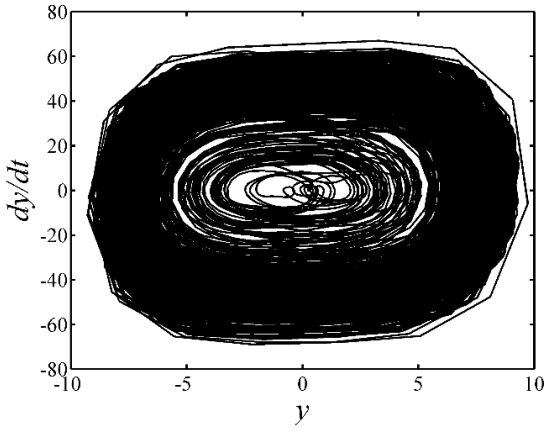

Figure 3.20: Phase diagram of out-of-plane mode with PR=0

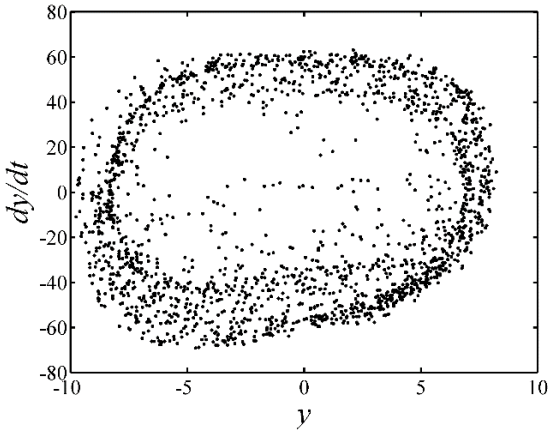

Figure 3.21: Poincare map of out-of-plane mode with PR=0

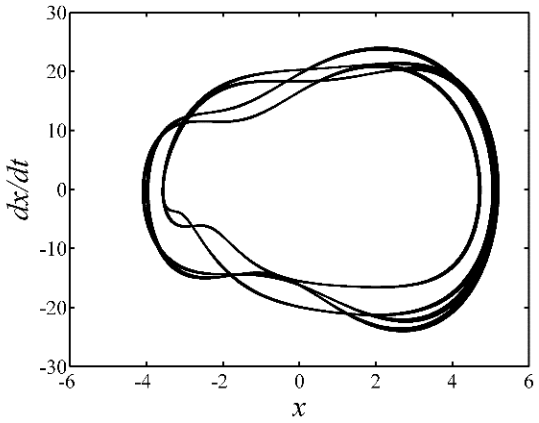

Figure 3.22: Phase diagram of in-plane mode with PR=0.47

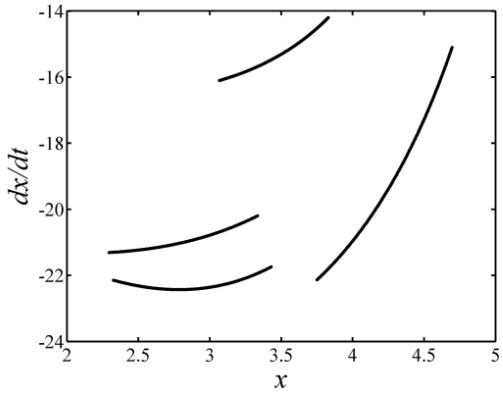

Figure 3.23: Poincare map of in-plane mode with PR=0.47

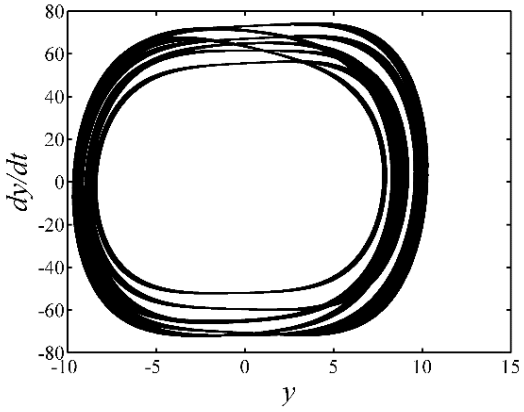

Figure 3.24: Phase diagram of out-of-plane mode with PR=0.26

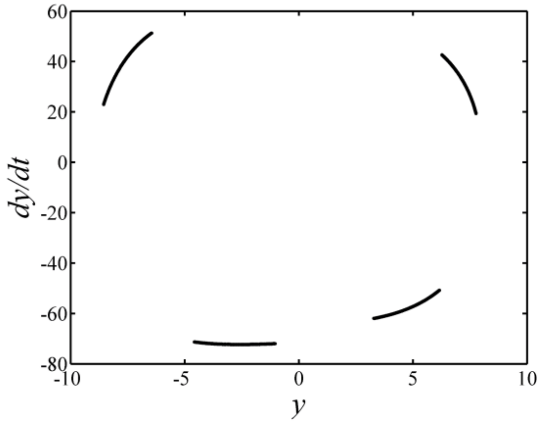

Figure 3.25: Poincare map of out-of-plane mode with PR=0.26

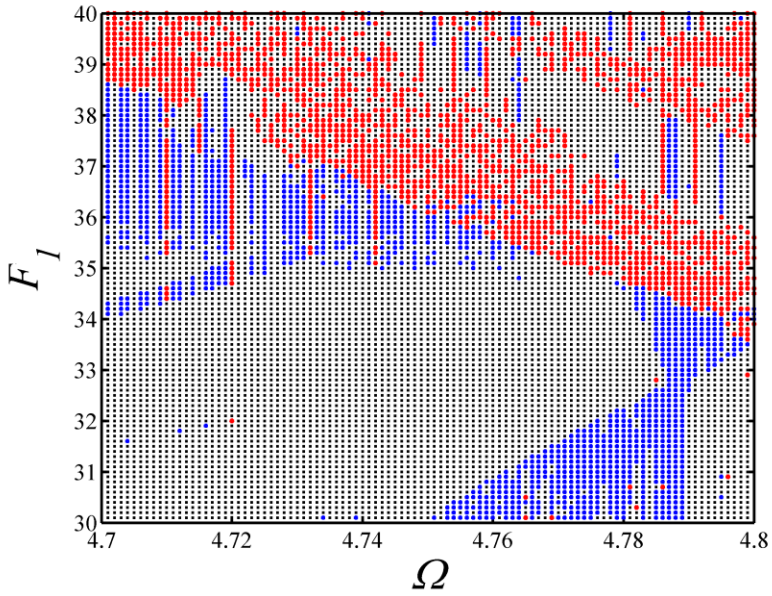

Figure 3.26: Periodic-nonperiodic-chaotic region diagram of in-plane mode of the cable

3.7 Conclusion and discussion

The nonlinear dynamic behavior of an elastic cable subjected to harmonic excitation in the tangential direction of equilibrium position of the table. Based on the second-order multi scale method, the derivation of an approximate periodic solution of the system is obtained and the analysis of stability of the solution is presented in this paper. The effect of different system parameters is studied. Chaotic motion of the system is found by simulation results. Based on the application of P-R method, a region diagram is given to study the influence of amplitude and frequency of excitation with ½ sub-harmonic resonance for the in-plane mode. From the results of the research, it can be concluded:

1. The steady-state solution of the in-plane and out-of-plane mode is increased monotonically with increase of f_1 and f_2 which are related to the force amplitude F.
2. The frequency response increase with the increase of natural frequency ω_x and ω_y.
3. As the cubic coefficients β_4 and β_1 increase, the system has the tendency to change from softening nonlinearity to hardening nonlinearity.
4. From the given region diagram which study the influence of excitation with the ½ sub-harmonic resonance for the in-plane mode, it can be obtained that, periodic motions appear near the ½ sub-harmonic resonance with a small excitation force. With the increase of amplitude of the excitation force, the system can be changed to chaotic motion.

As mentioned above, the coefficients are all defined by the properties of the cable. . Cases such as instability and chaos may cause collapse of the structure which should

be avoided in the design of structure. Study on influence of nonlinear parameters of the system can provide reference for the design of the structure. With application of the P-R method, this research is to reveal the nonlinear behavior of the suspended cable with considerations of large ranges of system parameters.

CHAPTER 4 NONLINEAR CHARACTERISTICS DIAGNOSIS BY COMBINING PERIODICITY-RATIO AND LYAPUNOV EXPONENTS METHODS

4.1 Introduction

Nonlinear dynamic systems widely exist in engineering applications. Nonlinear behaviors such as chaos may cause large and unpredicted displacements, it is therefore crucial in nonlinear dynamic analyses to effectively diagnose and distinguish different nonlinear characteristics of nonlinear systems. The efficiency and accuracy are also essential for diagnosing the nonlinear characteristics. Therefore, the criteria for distinguishing nonlinear motions such as periodic, quasiperiodic and chaos is needed and practically sound. Several diagnosing methods exist in the literature, which can applied to distinguish chaos from other nonlinear characteristics. Among the methods, Lyapunov exponent method is probably the widely used method in the field. The spectrum of the Lyapunov exponent has been proven to be one of the most accurate method to distinguish chaotic motions from regular motions (Nayfeh and Mook, 1988). The concept of the Lyapunov exponent method is based on evaluating the sensitivity of a system to initial conditions. The method provides a quantitative measure of the sensitivity. Numerous methods are found in the literature for determining the Lyapunov exponents. Wolf and Jack (1985) proposed a method of determining the Lyapunov exponent from a time series by monitoring the long-term growth rate of small volume elements in an attractor. Peter

(1995) proposed a method to calculate Lyapunov exponents for dynamic systems with discontinuities. The algorithm for the calculation of the spectrum of Lyapunov exponent is generalized for nonlinear dynamic systems with discontinuities. Other methods regarding to Lyapunov exponent methods were also study by numerous researchers to calculate the largest Lyapunov exponent and the system impact was also investigated (Blazejczky, 2001; Stefanski, 2003; Hinrichs,1997; Stefanski, 2003).

Even though the Lyapunov exponent method has been widely used method and proven to be an efficient method for diagnosing the nonlinear characteristics, it concentrates on the convergence and divergence of a nonlinear system, and the nonlinear behavior such as that of neither periodic nor chaotic characteristics cannot be diagnosed by the Lyapunov exponent method. In 1997, Dai and Singh proposed a method called P-R method to diagnose nonlinear characteristics of dynamic systems by introducing an index ranging between 0 and 1. The index named P-R value describes the periodicity of a system so the nonlinear characteristics of the system can be identified with different P-R values. Dai and Singh introduced the method with a study on the vibrations of a simple pendulum system. Dai and Wang (2008) compared the P-R method with the Lyapunov exponent method by defining the P-R value in a more accurate way. Dai and Han (2012) also applied the statistic hypothesis testing method to investigate the conditions of overlapping points.

As can be seen from the discussion above, the two methods of P-R and Lyapunov exponents show advantages and disadvantages. Typically, the Lyapunov exponent has difficulty in diagnosing the non-periodic and non-chaotic motions and the P-R method is incapable of distinguishing quasiperiodic from chaotic behaviors. This research intends to

establish a new method combining the two methods such that the advantages of the two methods can be maintained and the disadvantages of the methods can be eliminated. With the combination of Lyapunov exponent and P-R method, it is anticipated that the periodic, quasiperiodic, chaotic behavior and those in between the perfect periodic and chaotic responses of the systems can be diagnosed with higher efficiency and accuracy. To establish the combination method, it is necessary to understand the Lyapunov exponent and the P-R methods and identify their advantages and disadvantages.

4.2 Lyapunov exponent

4.2.1 Definition of Lyapunov exponent

Lyapunov Exponent of a dynamical system is used to measure the sensitive dependence upon initial conditions that is characteristic of chaotic behavior. The exponent indicates the average exponential rate of divergence or convergence of nearby trajectories in a phase diagram.

In the definition of the Lyapunov exponent, if a system is allowed to evolve from two slightly differing initial conditions, x and $x + \varepsilon$, where ε is a small number, then after n iterations of a numerical simulation, the divergence of the two systems can be characterized approximately as:

$$\varepsilon(n) \approx \varepsilon e^{\lambda n} \tag{4.1}$$

Where λ can be defined as the Lyapunov exponent which gives the average rate of divergence. Considering a nonlinear dynamic which can be described by a general equation:

$$x_{n+1} = f(x_n) \tag{4.2}$$

After n iterations, the difference between two initially nearby states can be written as:

$$f^n(x+\varepsilon) - f^n(x) \approx \varepsilon e^{\lambda n} \tag{4.3}$$

Where $f^n(x) = f\{f[\dots f[f(x)]\dots]\}$

Taking the natural logarithm of the equation, it can be obtained as:

$$\ln\left[\frac{f^n(x+\varepsilon)-f^n(x)}{\varepsilon}\right] \approx n\lambda \tag{4.4}$$

For small ε, the expression becomes

$$\lambda \approx \frac{1}{n}\ln\left|\frac{df^n}{dx}\right| \tag{4.5}$$

This a general expression of the Lyapunov exponent (Baker and Gollib), the chain rule is used for the derivative of the nth iterate and take the limit is taken as n tends to infinity to obtain:

$$\lambda = \lim_{n\to\infty}\frac{1}{n}\sum_{i=0}^{n-1}\ln|f'(x_i)| \tag{4.6}$$

4.2.2 Criterion to diagnose by Lyapunov exponent

A Lyapunov exponent is defined as the stretching rate per iteration, averaged over the trajectory of the system considered. If λ is negative, slightly separated trajectories converge and evolution is not chaotic. If λ is positive, nearby trajectories diverge, the evolution is sensitive to initial conditions and chaotic.

For an n-dimensional system there are n Lyapunov exponents, since stretching can occur for each axis, an n-dimensional initial volume is developed as:

$$V = V_0 e^{(\lambda_1+\lambda_2+\lambda_3)n} \tag{4.7}$$

For the continuous time dynamic system, the n-dimensional initial volume developed as:

$$V = V_0 e^{(\lambda_1+\lambda_2+\lambda_3)t} \tag{4.8}$$

For a dissipative system the sum of the exponents must be negative. If the system is chaotic then at least one of the exponents is positive.

Taking a driven pendulum system as an example, three Lyapunov exponents should be used to describe the three dimensions of the phase space $(\theta, \omega, \varphi)$ where θ is the phase angle, ω is the phase velocity, and φ is the initial phase angle. Since the orbits of the pendulum are the solutions to a set of differential equations governing the dynamic system, the calculation for the Lyapunov exponents is rather complicated. On a chaotic attractor, the directions of divergence and contraction are locally defined, and the calculation must be constantly adjusted. Despite this difficulty, many computer programs have been developed for calculating Lyapunov exponents. The Lyapunov exponent approach is not valid for diagnosing whether or not this system is periodic or chaotic if it cannot determine an expression for a dynamic system. The usual test for chaos with the utilization of the Lyapunov exponent is the calculation for the largest Lyapunov exponent. The largest positive Lyapunov exponent of a system is believed to indicate the corresponding system is chaotic. As an example, for a three-dimensional dissipative system, (0, −, −) of the Lyapunov exponents implies stable limit cycle, (0, 0, −) means quasiperiodic oscillation, and (+, 0, −) suggests a strange attractor of chaos (Carbajal-Gómez et al., 2013).

4.3 Periodicity-Ratio method

4.3.1 Concept of Periodicity-Ratio method

The P-R method was first introduced by Dai and Singh (1997) in their study of nonlinear dynamic systems for diagnosing periodic, quasi-periodic and chaotic responses of the systems. It can be used to efficiently identify the behaviors of motions for nonlinear dynamics by deciding the periodicity of the vibration system. An index between 0 and 1 is introduced to describe the periodicity of the system through an examination of the overlapping points in a Poincare map with respect to the total number of points generated by Poincare sections to create a Poincare map. As described by Dai (2008), nonlinear vibration motions such as periodic, nonperiodic, and chaotic motions can be distinguished with the P-R method.

It is well known that the Poincare map of a periodic system in a steady state consists of a finite number of visible points in the phase plane as described by Dai and Singh (1997). For periodic motion, each visible point in the Poincare map represents numerous points overlapping each other. However, for the chaotic case, the points in Poincare map only represent a few or even no overlapping points in the phase plane. Similarly, a quasiperiodic case also contain a negligibly small number of overlapping points. Actually, according to Dai (1995, 1997), the P-R value is the ratio of overlapping points to the total number of points. Therefore, for a periodic case, the P-R value equals to 1, and for a chaotic or a quasiperiodic case, the P-R value equals 0. The value must be greater than 0 but less than 1 when it comes to a nonperiodic case.

The P-R method considers the geometry of Poincare maps and describes the periodicity of the considered system. A general dynamic system subjected to an external excitation with period T can be implemented in detail. Assuming the solution of the considered system is $x(t)$ which represent a completely periodic solution for the system. Then the solutions of the periodic system should be a multiple of T rather than a single solution $x(t)$. In the other words, there must be other solutions satisfying the following expression:

$$x(t_0 + jT) = x(t_0) \tag{4.9}$$

where t_0 is a random vibration time and j is the number of periodic points in the corresponding Poincare map. T is the period of the system. If the system is completely periodic, no matter how large the time range is, there are numerous overlapping points for the point $x(t_0)$. However, the following equations must be satisfied to strictly define the overlapping points in the Poincare map:

$$X_{ki} = |X(\tau_0 + kT) - X(\tau_0 + iT)| \tag{4.10}$$

$$\dot{X}_{ki} = \left|\dot{X}(\tau_0 + kT) - \dot{X}(\tau_0 + iT)\right| \tag{4.11}$$

Where k is an integer in the range $1 \le k \le j$, i is an integer in the range $1 \le k \le n$ in which n is the total number of points generated for the Poincare map over the time range. The point $(x_i, \dot{x}_i)$ is regarded as an overlapping point of the k^{th} point $(x_k, \dot{x}_k)$ only if X_{ki} and $\dot{X}_{ki}$ all equal 0. The total number of the points overlapping the kth point in the corresponding Poincare map can be calculated with the following equation:

$$\zeta(\mathrm{k}) = \left\{\sum_{i=k}^{n} Q(X_{ki})Q(\dot{X}_{ki})\right\}P\left(\sum_{i=k}^{n}\left[Q(X_{ki})Q(\dot{X}_{ki})\right] - 1\right) \tag{4.12}$$

where $Q(y)$ and $P(z)$ are step functions expressed in the following form:

$$Q(y) = \begin{cases} 1, & if\ y = 0 \\ 0, & if\ y \neq 0 \end{cases} \tag{4.13}$$

$$P(z) = \begin{cases} 1, & if\ z = 0 \\ 0, & if\ z \neq 0 \end{cases} \tag{4.14}$$

In Eq. (4.12), ζ(k) is the number of overlapping points with the *k*th point in the Poincare map. In the other words, there are ζ(k) points which have identical displacement and velocity with the *k*th point. The equation developed for determining N, the total number of points can be expressed by

$$\mathrm{N} = \zeta(1) + \sum_{k=2}^{n} \zeta(k) P\left(\prod_{t=1}^{k-1}\{X_{ki} + \dot{X}_{ki}\}\right) \tag{4.15}$$

In which Π indicates the symbol for multiplication and P (.) is the step function as described previously. This equation describes the total number of overlapping points. The duplicated or missing calculations are prevented and only the overlapping points are calculated. Calculating Eq. (4.15) and the number of overlapping points can be obtained. If the system is periodic, all the points in Poincare map will be overlapping point and the P-R value will equal 1, the corresponding N in this case can be expressed in the following equation:

$$\mathrm{N} = \sum_{k=1}^{j} \zeta(k) \tag{4.16}$$

In this equation, the points in the Poincare map are classified by j sets, while the points in each set have the identical displacement and velocity. In this case, the points in the corresponding Poincare map are all overlapping points. As we described previously, the purpose of P-R method is to identify the periodicity through calculating the ratio of overlapping points to the total number of points in Poincare map. However, form the numerical analysis of a nonlinear system, not all points are periodic and in some cases, overlapping points may not necessarily be periodic points. Therefore, it is necessary to

distinguish the periodic points from overlapping points for the calculation of the P-R values.

4.3.2 Determining the periodic cases and the corresponding P-R values

To determine the number of periodic points, it is assumed that there are M sets of visible points on the surface of a Poincare map and *j* sets among these contain overlapping points no matter how many overlapping points it contains. It can be easily understood that among the j sets of points, some of the sets, considering the number p, will contain only few number of overlapping points. Eliminating the *p* sets of points, there are *j*=*M*-*p* set of points. The average time span of the overlapping points can be defined as:

$$\tau = \frac{t_{k,q} - t_{k,1}}{q-1} \tag{4.17}$$

where q represent the number of the overlapping points in the kth set, $t_{k,q}$ indicates the time when the *q*th overlapping point appear. In the kth set of points, each overlapping point may appear in everyτ time units. If we use a variance to determine how periodic the overlapping points will occur as following equation:

$$p^2 = \frac{\sum_i^{q-1}\left(t_{k,i+1} - t_{k,i} - \tau\right)^2}{q-1} \tag{4.18}$$

If the p^2 equals to 0 or is small enough, the overlapping points in the kth set are completely periodic.

Consider the kth group of overlapping points among the j groups, the time span between the *i*th point in the kth group and the i+1th point in the same group can be defined as:

$$T\_(k,i) = t\_(k,i+1) - t\_(k.i) \tag{4.19}$$

And the time span between the $(i+2)th$ point and the $(i+1)th$ point can be described:

$$T_{k,i+1} = t_{k,i+2} - t_{k.i+1} \tag{4.20}$$

If the overlapping points in the kth group satisfy the following equation:

$$T_{k,i} - T_{k,i+1} = 0 \tag{4.21}$$

Then the $i, i+1, i+2$ points are periodic points. The number of periodic points with an identical time span in the kth group can be determined by employing the following formula:

$$\zeta(k) = \left\{\sum_{h=i}^{q-1} Q\left(T_{k,h} - T_{k,h+1}\right)\right\} P\left(\sum_{h=i}^{q-1} Q\left(T_{k,h} - T_{k,h+1}\right) - 1\right)$$

$$+P\left(Q\left(\sum_{h=i}^{q-1} Q\left(T_{k,h} - T_{k,h+1}\right) - 1\right)\right) \tag{4.22}$$

in which the $Q(.)$ and $P(.)$ are the step function as describe previously. The total number of periodic points in the *k*th group can be calculated with the following equations:

$$\Phi(k) = \zeta(1) + \sum_{i=2}^{q-1} \zeta(i)\, P\left(\prod_{h=1}^{i-1}\left\{T_{k,i} + T_{k,h}\right\}\right) \tag{4.23}$$

The total number of periodic overlapping points (denoted as NPP) among the entire points in the Poincare map is expressible as:

$$\mathrm{NPP} = \zeta(1) + \sum_{k=1}^{j} \phi(k) \tag{4.24}$$

the P-R value can then be defined as:

$$\gamma = \lim_{n\to\infty} \frac{NPP}{n} \tag{4.25}$$

If the dynamic system is completely periodic, all the points in the Poincare map are overlapping points, and the P-R value should equal to 1. The system will be quasi-periodic or chaotic if γ equals 0. The P-R value is therefore an index quantifying the periodicity of a nonlinear dynamic system. Based on the P-R method, the nonlinear behavior such as periodicity, quasiperiodicity, chaos and other nonlinear behavior of a nonlinear system can be easily diagnosed.

In addition, what have to be mentioned is that the overlapping boundary is also a significant consideration for defining the periodic overlapping points and P-R value. Such research has been conducted by Dai and Han (2011). In the study of Duffing's equation, the influence of overlapping boundaries on the P-R values was studied. It can be concluded that when the overlapping boundary is smaller than 10^{-3}, the portion occupied by chaos remains almost constant. Therefore, in the following numerical simulation of the region diagram by P-R method, the overlapping boundary is set as 5×10^{-4}.

4.4 Comparison of the Lyapunov exponent and P-R method

To demonstrate the P-R method and compare it with the Lyapunov exponent method which has been widely used in diagnosing chaotic motions of dynamic systems, the Duffing's equation in the following form which has been studied by Ueda and other researchers is considered in this research:

$$\ddot{x} + K\dot{x} + x^3 = B\cos t \tag{4.26}$$

In Ueda's studies, a wide variety of periodic and chaotic behaviors were obtained corresponding to a relatively larger range of system parameters k and B. A periodic-chaotic region diagram was presented by Ueda the first time. A much detailed and more accurate periodic-quasiperiodic-chaotic region diagram was reported by Dai and Singh (1997) with employment of a single value criterion, the P-R value, for diagnosing the nonlinear behavior of the system. In this research, to compare the P-R method and Lyapunov method and establish a new method combining the two methods, several such region diagrams are generated as per the two methods. Figure 4.1 shows a periodic-nonperiodic region diagram generated by using the P-R method. In the diagram, the crosses represent periodic cases and the stars are the states of nonperiodic cases including chaotic and quasiperiodic responses of the system. The region diagram plotted by P-R method meets well with that shown in literature, though the quasiperiodicity of the system needs to be diagnosed with the other approaches.

A similar diagram is generated per the Lyapunov method as shown in Figure 4.2. In the diagram, the crosses are for nonchaotic cases and the stars are for the chaotic cases of the system. As Lyapunov exponent is a widely used criterion for diagnosing chaos, Figure 4.2 illustrates the chaotic and nonchaotic cases of the system.

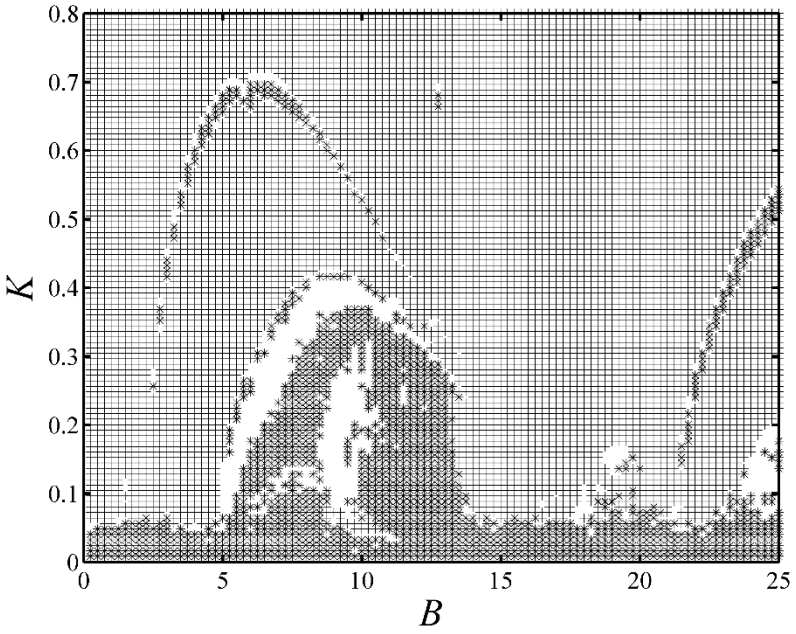

Figure 4.1: Periodic-nonperiodic region diagram plotted by P-R method

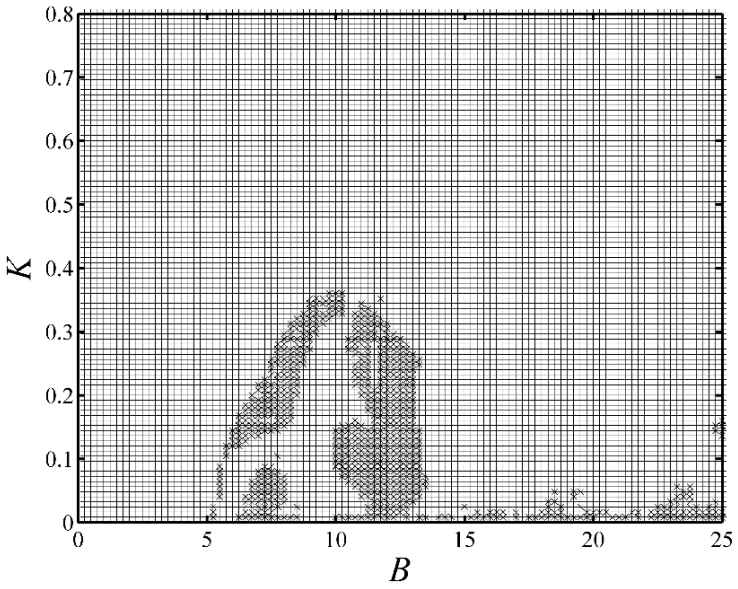

Figure 4.2: Chaotic-nonchaotic region diagram plotted by Lyapunov exponent method

In the research work of Dai and Singh (1997), the periodicity ratio was defined as overlapping points to the total points in the Poincare map. However, as described previously, the new definition described above for the periodicity ratio considers periodically overlapping points and uses the ratio of periodically overlapping points and total points in a Poincare map to define the P-R value. Comparing the region diagrams, there are several different cases can be observed. To verify the accuracy of the new definition, the results of the two approaches with the old and new definition for the P-R values are compared. Figure 4.3 and Figure 4.4 show the phase diagram and Poincare map of a case of which B=2, and K=0.016. As per the old definition, the P-R value is between 0 and 1 which means an irregular case, neither periodic nor chaotic. However, based on the new definition considering the periodically overlapping points, the P-R value for this case is calculated as 0, which is a quasiperiodic case or a chaotic case. From the phase diagram and Poincare map corresponding to this case, it can be concluded that this is indeed a quasiperiodic case. Figure 4.5 shows the Lyapunov exponents of the selected case with Lyapunov exponents 0, $-0.74 \times 10^{-4}, 0.86 \times 10^{-4}$, which also indicates a quasiperiodic case. This implies that the new definition is more accurate in diagnosing nonlinear motions and should be adapted in determining for the P-R values. It should be noticed however, based on the calculations for the system considered; most of the results found by employing the old definition are identical to that of the new definition.

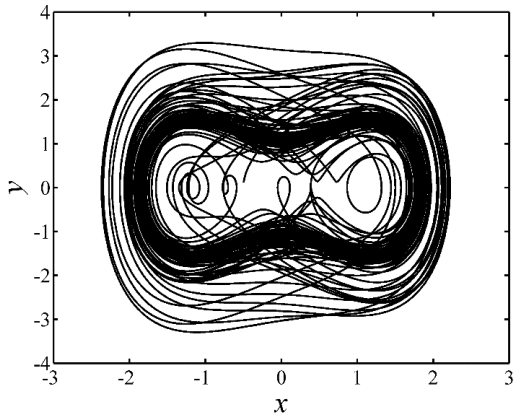

Figure 4.3: Phase diagram of the system with K=0.016, B=2

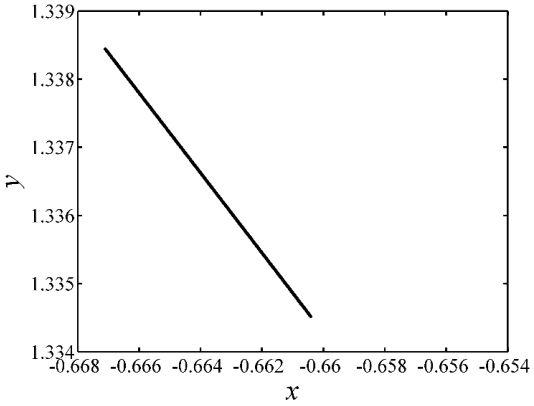

Figure 4.4: Poincare map of the system with K=0.016, B=2

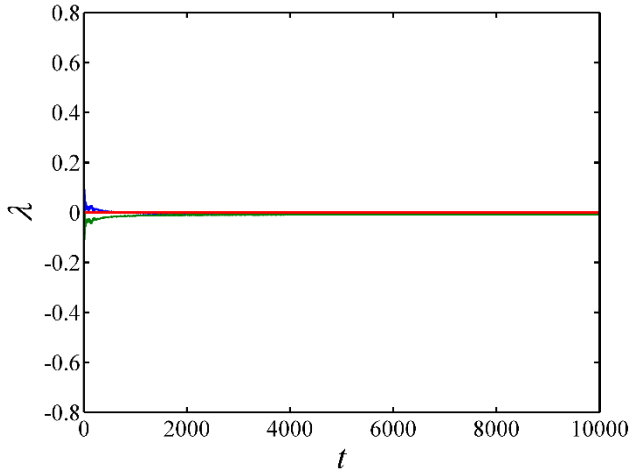

Figure 4.5: Lyapunov exponents of the system with B=2, K=0.016

4.4.1 Comparison of nonlinear motions in region diagrams

As can been seen in the Figure 4.1 and Figure 4.2, most of the cases calculated by the two methods are in good agreement with each other, especially for the perfect periodic and chaotic cases. However, there are still some different non-periodic regions. The following discussion part is classified into three parts.

(1) Perfectly agreed areas. It can be easily seen from the two Figures area such as K=0.024-0.15, B=11-13.5, in this area, the nonlinear can be regarded as chaotic motions based on the numerical calculations for the system by two method. A selected case can be seen in the Figure 4.6-Figure 4.8 with B=12, K=0.1., Figures 4.6 and 4.7 are the phase diagram and Poincare map of the dynamic system respectively. It can be easily distinguished from the phase diagram and Poincare map that the system is chaotic under the condition B=12 and K=0.1. Figure 4.8 indicates the Lyapunov exponents for the system. As can be seen form the Figure, the largest Lyapunov exponent is 0.1435 which is a positive value. According to the criterion, a positive largest Lyapunov exponent indicates a chaotic motion which agrees well with the phase diagram and Poincare map. However, as calculated by P-R method, the P-R value equals to 0 which also represent a chaotic case. In this case, P-R method is in good agreement with the Lyapunov exponent method.

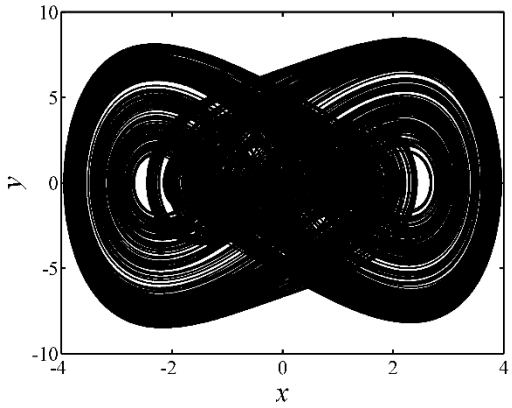

Figure 4.6: Phase diagram of the system with B=12, K=0.1

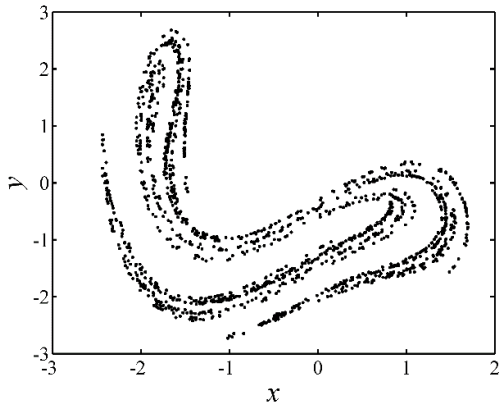

Figure 4.7: Poincare map of the system with B=12, K=0.1

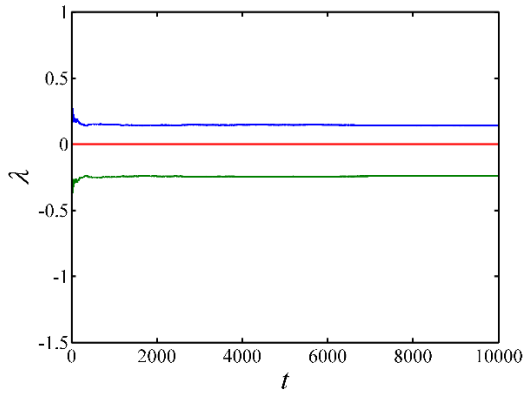

Figure 4.8: Lyapunov exponents of the system with B=12, K=0.1

(2) Partially agree areas. In these areas, the results obtained by Lyapunov exponent method and P-R method partly agree with each other. From the region diagrams above, it can be easily observed that in the areas such as B=5-10 and K= 0-0.35. Since the agreed cases have been discussed above, therefore, in this section, some different points are selected to implement the characteristics of the two methods. Figures 4.9-4.11 show the phase diagram, Poincare map and the Lyapunov exponents of the case where B=6 and K=0.25. Under this condition, the calculated P-R value is 0.4997. From the Poincare map, the motion of the system is an irregular case but close to the periodic case. However, from the Figure 4.9 in which the Lyapunov exponents are 0, -0.0015, -0.2104, the motion is periodic. From the description above, there exist many irregular motions in between period and chaos, and it can be seen from Figure 4.2 that the Lyapunov exponent is unable to distinguish them from periodic and chaos. However, the concept of P-R value is to describe the periodicity of a vibration system, and it is superior in this aspect.

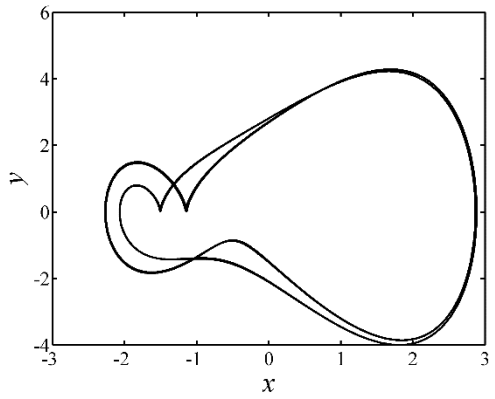

Figure 4.9: Phase diagram of the system with B=6, K=0.25

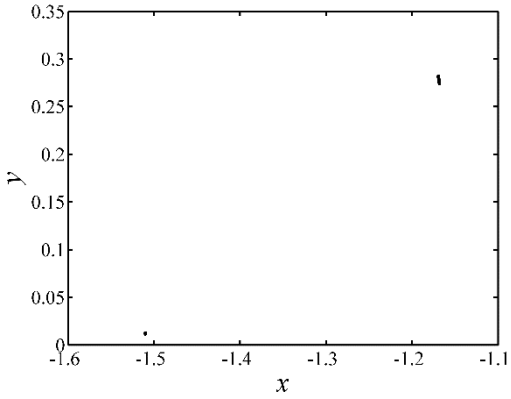

Figure 4.10: Poincare map of the system with B=6, K=0.25

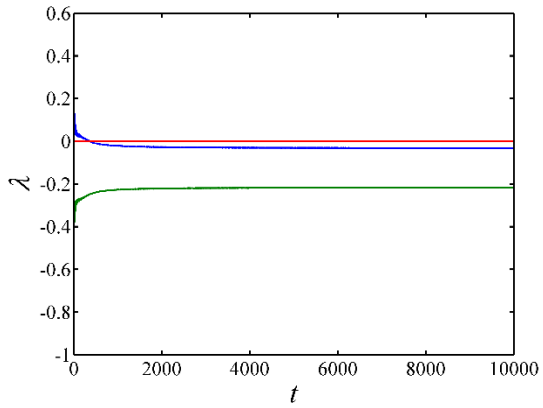

Figure 4.11: Lyapunov exponents of the system with B=6, K=0.25

(3) Disagree areas. The areas such as B=0.032-0.15 and K=23.5-25 in the region diagrams plotted by the Lyapunov exponent and P-R methods disagree with each other. Figures 4.12-4.15 show a disagreed case with B=23.75 and K=0.1, with the calculated results, the P-R value equals to 0 which may indicate a chaotic or quasiperiodic case. From the response as shown in the corresponding phase diagram and Poincare map, Figures 4.14 and 4.15, it can be seen that the system is a chaotic case. For further verifying this conclusion, a Fast Fourier transform diagram is plotted for this case as shown in Figure 4.16. Fast Fourier transform is a discrete Fourier Transform which reveals the periodicity of the input data and the relative strength of any periodic components (Naussbaumer,1982). The horizontal axis of the Figure 4.16 indicates the frequency of the periodic components and vertical axis indicates amplitude of periodic components. From the fast Fourier transform diagram, as per the spectral analysis (Naussbaumer,1982) it can be concluded that there exist numerous periodic solutions with different amplitudes and frequencies in a time history which is an important characteristic of a chaotic case. However, as shown in Figure 4.15, the three Lyapunov exponents are 0,-,-, which indicates a periodic case instead. The reason Lyapunov exponent does not give correct prediction is that the Lyapunov exponent actually describes divergence or convergence of a system. From the response of the case, it can be seen that even though the displacements of the system are different along the time series, but the characteristics such as amplitudes and shape of the wave curves are not varying significantly time increases. Although the points in the Poincare map are indeed spread and form a few “clouds” as shown in Figure 4.14, the clouds are localized and the areas of the clouds are relatively small. Therefore, in the calculation by Lyapunov exponent

method, the system is regarded as a periodic case. This is to say that not all the converged cases are periodic cases (Henon,1976).The P-R method has describes the periodicity of the considered system and the zero P-R value for this case indicates that the system has no periodicity at all and the response of the system is chaos for this case, as shown in the phase diagram and Poincare map Figures 4.13 and 4.14.

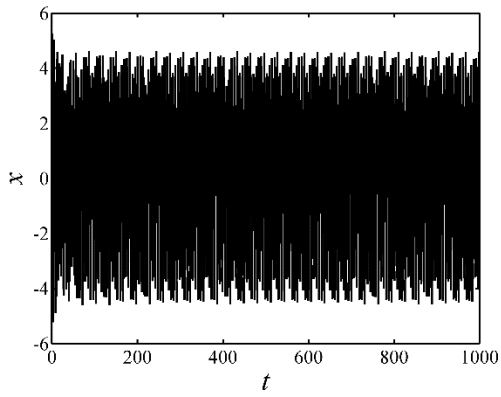

Figure 4.12: Dynamic response of the system with B=23.75, K=0.1

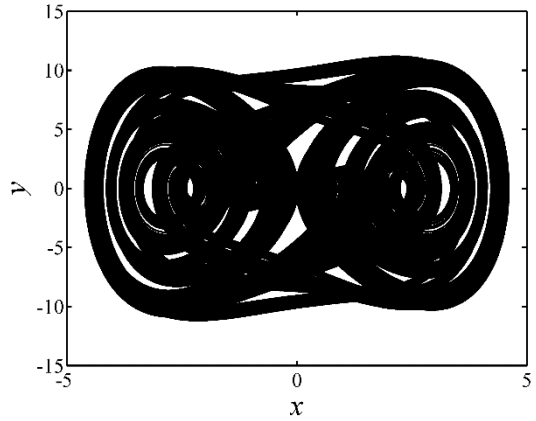

Figure 4.13: Phase diagram of the system with B=23.75, K=0.1

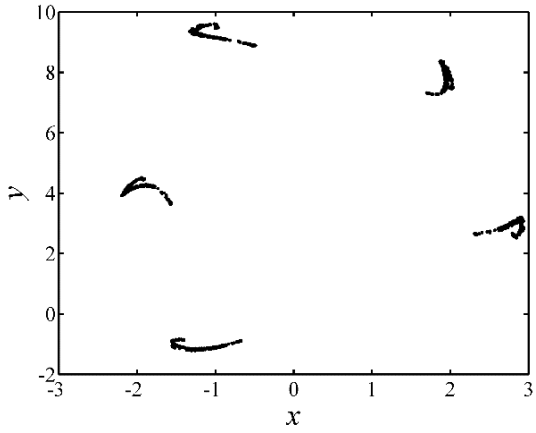

Figure 4.14: Poincare map of the system with B=23.75, K=0.1

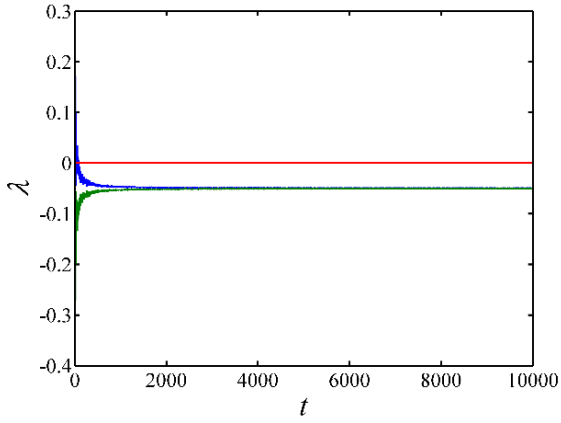

Figure 4.15: Lyapunov exponents of the system with B=23.75, K=0.1

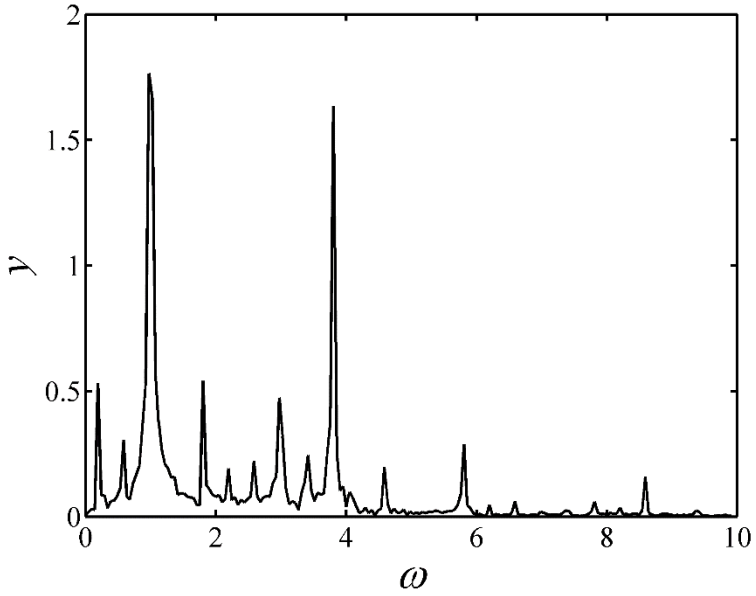

Figure 4.16: Fast Fourier Transform for the case of K=0.1, B=23.75

4.4.2 Comparison of calculation time

The simulation times of the region diagrams for each method are compared. In the simulated procedure, one may notice that the simulation time for the Lyapunov exponent is much larger than that for P-R method. Table 4.1 shows the CPU time for random points calculated by the two methods. It can be noticed that if the system is converged, then the calculation time for one point by two methods is almost the same. However, when it comes to the diverged cases, the calculation time by Lyapunov exponent is much more than that by P-R method. The reason for that is that the calculation for Lyapunov exponent mainly focuses on obtaining three stable Lyapunov exponents. Nonlinear behavior then can be diagnosed according to values of Lyapunov exponents. However, for some cases, even a periodic case may cost a lot of time to obtain a stable Lyapunov exponent, resulting in the inefficiency of the method. In addition, in the procedure of calculation of region diagrams, the calculation time must be set constantly for every points, resulting in longer calculation time for Lyapunov exponent method. Table 4.2 show the rough CPU time for the calculation of region diagrams by the two methods respectively. It can be noticed that the calculation time by Lyapunov exponent is about three times that by P-R method which show the efficiency of P-R method. Therefore, for studying the nonlinear behavior of the system in large range of system parameters, P-R method is more efficient than Lyapunov exponent method.

Table 4. 1: Time comparison for one point

Method	CPU time (second)
Periodicity Ratio	4.414
Lyapunov exponent (convergence)	4.521
Lyapunov exponent (divergence)	15.427

Table 4. 2: Time comparison for region diagrams

Method	CPU time (hours)
Periodicity Ratio	24
Lyapunov exponent	75

4.5 Periodic-quasiperiodic-chaotic region diagram by combination of the two methods

In the previous discussion, it can be concluded that P-R method has superiority in diagnosing periodic cases and nonlinear cases. However, it has difficulty in distinguish quasiperiodic from chaotic cases, for they have the identical P-R value of zero. On the other hand, the Lyapunov exponent method is incapable of diagnosing some of the non-chaotic cases of the system. Nevertheless, the Lyapunov exponent method shows advantage on distinguishing quasiperiodic cases from chaos. Figures 4.17-4.19 show the phase diagram and Poincare map of a quasiperiodic case with a P-R value 0. From the given Lyapunov exponents figure, the three Lyapunov exponents are $-3.8 \times 10^{-4}, 0, -3.8 \times 10^{-4}$,which indicate a quasiperiodic case, agreeing with the Poincare map as shown in Figure 4.18. Therefore, it can be expected, all the nonlinear behavior such as periodic, quasiperiodic, chaotic, and irregular motions in between periodic and chaotic cases can be distinguished by combing the two methods,.

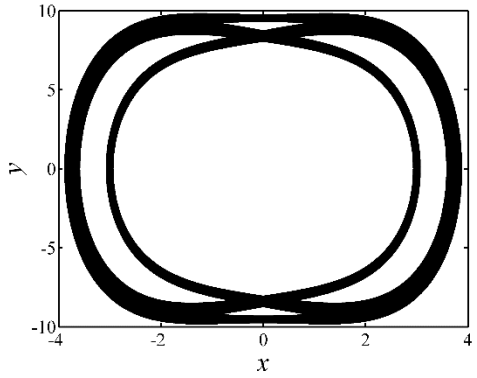

Figure 4.17: Phase diagram of the system with B=5.25, K=0.001

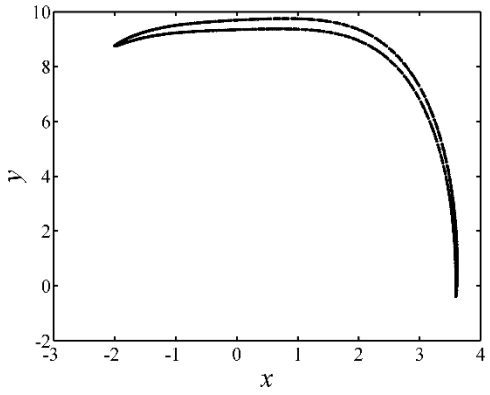

Figure 4.18: Poincare map of the system with B=5.25, K=0.001

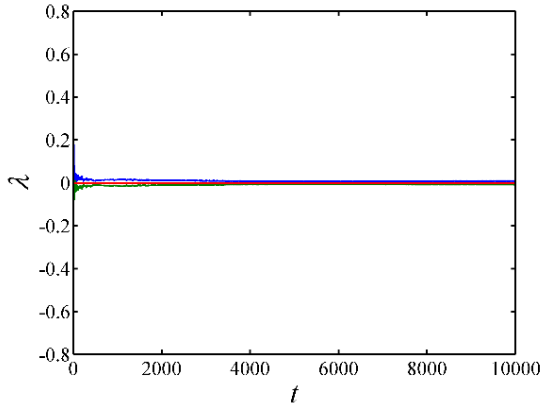

Figure 4.19: Lyapunov exponents of the system with B=5.25, K=0.001

Based on the discussion above, more accurate and efficient diagnosis for the nonlinear behaviors of the system can be expected if the two methods of P-R and Lyapunov exponent can be combined. In this research, the P-R method is used to diagnose the periodic and nonperiodic cases for the system, especially the nonlinear cases which are neither periodic nor chaotic, and the Lyapunov exponent method is employed to distinguish quasiperiodic cases from the cases of which the P-R values are zeros. The results obtained are shown in Figure 4.20 which shows a periodic-quasiperiodic- chaotic region diagram, given by combining of the Lyapunov exponent and P-R method. In the figure, the plus sign indicates the points where P-R value equals to 1, in other word, a case of periodic motion. The diamond represents the point with a P-R value equals to 0 which indicates that the nonlinear motion is a quasiperiodic motion. The blank areas are composed of irregular motions which have P-R values in between 0 and 1. The solid points represent chaotic cases. Such a region diagram give a global picture of dynamical behavior of considered system within a large rang of parameter values.

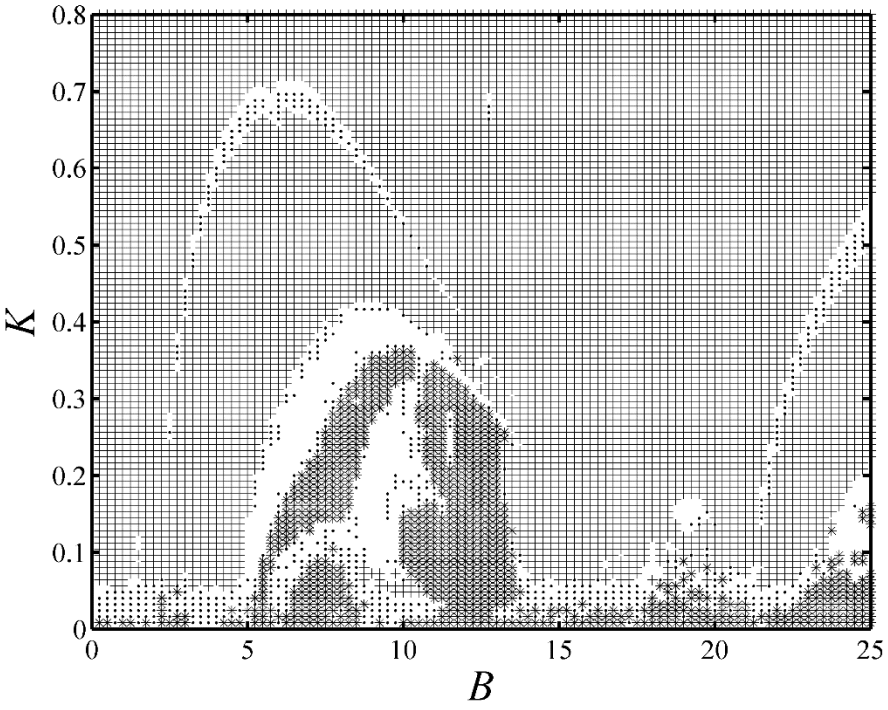

Figure 4.20: Periodic-quasiperiodic-chaotic region by combining the Lyapunov exponent method and P-R method

To check the accuracy of this diagnosis method combining the two methods of P-R and Lyapunov method, a quasiperiodic case in the Figure 4.18 with K=0.65, B=5 is selected. Figure 4.21 shows the phase diagram of the system, and Figure 4.22 is the Poincare map. The case can be seen indeed a quasiperiodic, from these two Figures. It meets well with Figure 4.23 which indicates the Lyapunov exponents of the system.

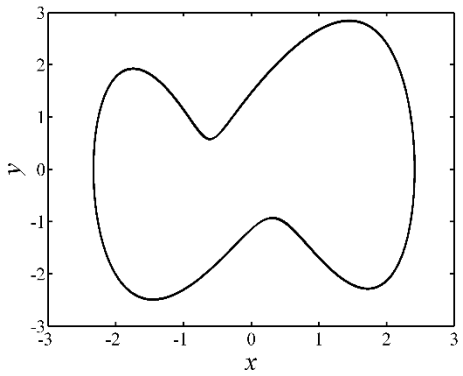

Figure 4.21: Phase diagram of the system with B=5, K=0.65

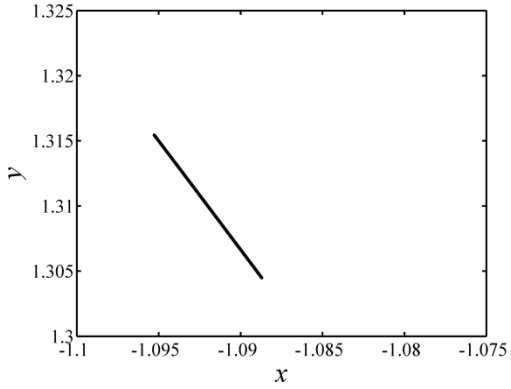

Figure 4.22: Poincare map of the system with B=5, K=0.65

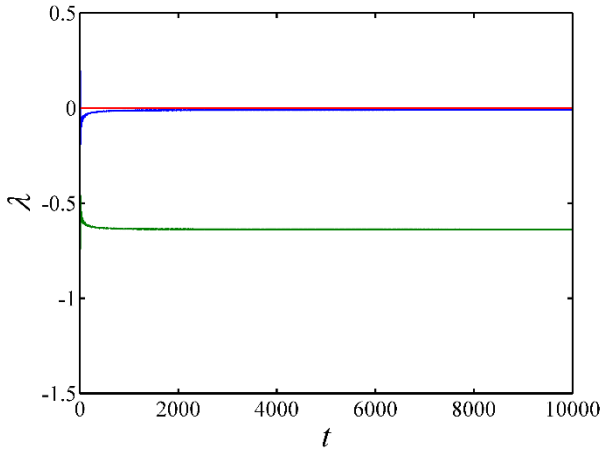

Figure 4.23: Lyapunov exponent of the system with B=5, K=0.65

In comparing with Figures 4.1 and 4.2, the region diagrams generated by merely the P-R method or Lyapunov exponent method, Figure 4.20 created by the new method combining the two methods is much more accurate and reliable. The quasiperiodic cases are accurately diagnosed as per the Lyapunov method; the cases inaccurately identified by the Lyapunov method are eliminated as per the results of the P-R method; and the periodic, nonperiodic and chaotic cased are characterized by the P-R method. Significantly, the nonlinear cases in between perfect periodic and chaotic cases are identified. This periodic-quasiperiodic-chaotic region diagram is therefore ready to use for analyzing nonlinear behaviors of the system. The method established in the research is therefore not only more accurate and efficient in comparing with merely employing the P-R method or Lyapunov exponent method but also practically sound.

4.6 Conclusions

As can be seen from the discussion above, both the Lyapunov exponent and P-R method have disadvantages and advantages. In this research, the comparison of the two method are conducted and following conclusions can be obtained:

1. The P-R method describes how periodic of a system is. With the introducing of an index namely the P-R value which is a value in between 0 and 1, the periodicity of a system can be quantitatively described.
2. With the new definition considering the periodically overlapping points in a Poincare map, the nonlinear motions can be diagnosed more accurately.
3. From the region diagrams plotted by Lyapunov exponent method and P-R method, it can be seen that both the two methods can diagnose nonlinear behavior. However, regarding to the calculation time, P-R method is more efficient.

4. With application of P-R method, the irregular motions which between periodic and chaotic can be diagnosed. However, Lyapunov exponent method is incapable to distinguish them.
5. For some cases which are diagnosed as periodic by Lyapunov exponent method, the phase diagram and Poincare map show chaotic case. It can be concluded that not all the converged cases are periodic. However, from describing the periodicity of the system, they can be diagnosed accurately by P-R method.
6. The Lyapunov exponent method has advantages in diagnosing quasiperiodic motion. With the combination of the two methods, all the nonlinear behavior can be distinguished within a large rang of system parameters.

CHAPTER 5 CONCLUSIONS AND FUTURE WORK

5.1 Conclusions

Research results have been obtained from analyzing theoretical and numerical simulations and diagnosing the nonlinear behavior of a cable subjected to parametric excitations. The results and conclusive findings are listed as follows:

1. In the study of vibration of a fixed-free cable considered in this research using perturbation method, the steady-state solution of in-plane and out-of-plane mode will increase monotonically with the increase of f_1 and f_2 which are related to the force amplitude F. With the increase of the excitation amplitude F, the response of the vibration system increase correspondingly.
2. The natural frequencies of both in-plane mode and out-of-plane modeω_x and ω_y have a positive relation with the dynamic response. With the increase the natural frequencies, the steady-state solution of the dynamic cable increase and the unstable regions increase as well. However, the increase of both response and unstable region is not significant.
3. From the investigation of the influence of system coefficients, it can be obtained if the cubic coefficient β_4 for in-plane mode increase, the response of the in-plane mode increase as well and the system has a tendency to change from softening nonlinearity to hardening nonlinearity. Similarly, as the increase of the nonlinear coefficient β_1, the response of the out-of-plane mode increase.
4. From the given region diagram which study the influence of excitation with the ½ sub-harmonic resonance for the in-plane mode, it can be obtained that, periodic

motions appear near the ½ sub-harmonic resonance with a small excitation force. With the increase of amplitude of the excitation force, the system can be changed to chaotic motion. Comparing the region diagram, the accuracy of the stability analysis can be guaranteed.

5. By applying the P-R method, a periodic-nonperiodic-chaotic region is given to show the influence of frequency and amplitude of the external excitation within a large range of system parameters.
6. P-R method is used to describe how periodic of a system. With the introducing of an index between 0 and 1, the periodicity of a system can be obtained.
7. With the new definition for the P-R value, the nonlinear motions can be diagnosed more accurately.
8. From the region diagrams plotted by Lyapunov exponent method and P-R method, it can be seen that both the two methods can diagnose nonlinear behavior. However, regarding to the calculation time, P-R method is more efficient.
9. With application of P-R method, the irregular motion which between periodic and chaotic can be diagnosed. However, Lyapunov exponent method is incapable to distinguish them.
10. For some cases which are diagnosed as periodic by Lyapunov exponent method, the phase diagram and Poincare map show chaotic case. It can be concluded that not all the converged cases are periodic. However, from describing the periodicity of the system, they can be diagnosed accurately by P-R method.
11. The Lyapunov exponent method has advantages in diagnosing quasiperiodic motion.

12. The new approach of combing both the P-R and Lyapunov exponent methods for diagnosing the nonlinear behavior of a dynamic system, the results of the diagnosis are much more accurate and reliable with integration of the advantages of the two methods.

5.2 Future work

5.2.1 Nonlinear study on flexible structures

The research mainly focuses on the nonlinear behavior of cables subjected to harmonic excitation, however, in engineering applications, the excitations are more complicated. Recommendations for future work include a study of nonlinear behavior induced by complicated excitations such as wind and fluid excitations. Advanced simulation methods should be proposed to make it as close to reality as possible. Another aspect of future research may focus on the interaction between structures and moving loads such as moving vehicles.

5.2.2 Predictability of nonlinear behavior

Complicated nonlinear systems may have paradoxical regions such as tendencies toward divergence and convergence. All of the complicated regions are difficult to predict. As is well-known, nonlinear behavior such as chaos may cause heavy losses in engineering. If system predictability can be used to characterize chaos, then the system parameters which induce chaos can be avoided. Future work may focus on a predictability index to predict behavior for a nonlinear system.

BIBLIOGRAPHY

I. Kovacic and M. Brennan, The duffing equation: nonlinear oscillators and their behavior, 1st Ed., Wiley, Chichester, 2011.

S. Rinaldi and S. Muratori, Conditioned chaos in seasonally perturbed predator-prey models, *Ecological Modelling* 69, 79-97 (1993).

S. Rinaldi, S. Muratori and Y. Kuznetsov, Multiple attractors, catastrophes and chaos in seasonally perturbed predator-prey communities, *Bulletin of Mathematical Biology* 55, 15-35 (1993).

S. S. Rao, Mechanical vibration. 3rd edition. Reading, MA, Addison-Wesley Publishing Company (1995).

S. Gakkhar and R. Naji, Chaos in seasonally perturbed ratio-dependent prey-predator system, *Chaos, Solitons and Fractals* 15, 107-118 (2003a).

P. Hagedorn and B. Schafer, On non-linear free vibrations of an elastic cable, *J. Non-Linear Mech* 15, 333 (1980).

A. Luongo, G. Rega and F. Vestroni, Oscillations of a non-linear model of a suspended cable. *J. Sound Vib* 82. 247 (1982).

G. Rega. F. Vestroni and F. Benedettini, Parametric analysis of large amplitude free vibrations of a suspended cable, *J. Solids Struct.* 20. 95 (1984).

N. Perkins, Modal interactions in the non-linear response of elastic cables under parametric/external excitation. *International Journal of Non-linear Mechanics* 27, 233–250 (1992).

F. Benedettini, G. Rega, and R. Alaggio, Non-linear oscillations of a four-degree-of-freedom model of a suspended cable under multiple internal resonance conditions. *Journal of Sound and Vibration* 182, 775–798 (1995).

M. Pakdemirli and A. Nayfeh, Analysis of one-to-one autoparametric resonances in cables: discretization versus direct treatment. *Nonlinear Dynamics* 8, 65–83 (1995).

G. Rega, W. Lacarbonara, A. Nayfeh and C. Chin, Multiple resonances in suspended cables: direct versus reduced-order models. *International Journal of Non-linear Mechanics* 34, 901–924 (1999).

W. Chang, R. Ibrahim, and A. Afaneh, Planar and non-plane non-linear dynamics of suspended cables under random in-plane loading—I. Single internal resonance. *International Journal of Non-linear Mechanics* 31, 837–859 (1996).

L. Martinelli, and F. Perotti, Numerical analysis of the non-linear dynamic behavior of suspended cables under turbulent wind excitation. *International Journal of Structural Stability and Dynamics* 2, 207–233 (2001).

A. Nayfeh, A. Arafat, C. Chin and W. Lacarbonara, Multimode interactions in suspended cables. *Journal of Vibration and Control* 8, 337–387 (2002).

S. Nielsen and P. Kirkegaard, Super and combinatorial harmonic response of flexible elastic cables with small sag. *Journal of Sound and Vibration* 251, 79–102 (2002).

H. Arafat and A. Nayfeh, Non-linear responses of suspended cables to primary resonance excitations. *Journal of Sound and Vibration* 266, 325–354 (2003).

V. Gattulli and M. Lepidi, Nonlinear interactions in the planar dynamics of cable-stayed beam. *International Journal of Solids and Structures* 40, 4729–4748 (2003).

H. Chen and Q. Xu, Bifurcations and chaos of an inclined cable. *Nonlinear Dynamics* 57, 37-55 (2009).

P. Warnitchai, Y. Fujino, and T. Susumpow, A non-linear dynamic model for cables and its application to a cable–structure system. J. *Sound and Vibration* 187 695–712 (1995).

H. Swinney, Observations of order and chaos in nonlinear systems, *Physica* 7D (1983).

J. C. Roux, R.H. Simoyi and H. L. Swinney, Observation of a strange attractor, *Physica* 8D 257 (1983).

B. Malraison, P. Atten, P. Berge and M. Dubois, Turbulence-dimension of strange attractors: an experimental determination for the chaotic regime of two convective systems, *J. Physique Lettres* 44 (1983).

J. Guckenheimer and G. Buzyna, Dimension measuremerits for cjeostrophic turbulence, *Phys. Rev. Lett*. 51, 1438 (1983).

J. Gollub, E. Romer and J. Socolar, Trajectory divergence for coupled relaxation oscillators: measurements and models. *J. Stat. Phys*. 23, 321 (1980).

P. Muller, Calculation of Lyapunov exponents for dynamical systems with discontinuities. *Chaos, Solitons & Fractals* 5(9),1671-81 (1995).

F. C. Moon, Chaotic Vibrations, Wiley, New York, 1987.

F. C. Moon, Experiments on chaotic motions of a forced nonlinear oscillator: Strange attractors, ASME *J. Appl. Mech.* 47, 638–644 (1980).

A. Wolf, J. B. Swift, H. L. Swinney, and J. A. Vastano, Determining Lyapunov exponents from a time series. *Physica* D 16, 285–317 (1985).

G. L. Backer and J. P. Gollub, Chaotic Dynamics, Cambridge U. P., Cambridge, England, 1990.

V. Carbajal-Gómez, E. Tlelo-Cuautle and F. Fernández, Optimizing the positive Lyapunov exponent in multi-scroll chaotic oscillators with differential evolution algorithm. *Applied Mathematics and Computation* 219, 8163-8168 (2013).

D. Souza and I. Caldas, Calculation of Lyapunov exponents in systems with impacts. *Chaos, Solitons & Fractals,* 23(3), 569–79 (2004).

A. Stefanski, Estimation of the largest Lyapunov exponent in systems with impacts. *Chaos, Solitons & Fractals,* 11,2443–51 (2000).

A. Stefanski and T. Kapitaniak, Estimation of the dominant Lyapunov exponent of non-smooth systems on the basis of maps synchronization. *Chaos, Solitons & Fractals* 15, 233–44 (2003).

J. D. Farmer, E. Ott, and J. A. Yorke, The dimension of chaotic attractors. *Physica* D 7, 153–170 (1983).

Y. Ueda, Steady motions exhibited by Duffing's equations: A picture book of regular and chaotic motions. *New Approaches to Nonlinear Problems in Dynamics*, edited by P. J. Holmes ~SIAM, Philadelphia, 311–322 (1980).

L. Dai and M. C. Singh, On oscillatory motion of spring-mass systems subjected to piecewise constant forces. *J. Sound Vib* 173, 217–231 (1994).

L. Dai and M. C. Singh, An analytical and numerical method for solving linear and nonlinear vibration problems, *Int. J. Solids Struct* 34, 2709–2731 (1997).

S. Ciliberto and J. P. Gollub, Chaotic mode competition in parametrically forced surface waves, *J. Fluid Mech.,* 158, 381–398 (1985).

H. Zhang, T. Huang and L. Dai, Nonlinear dynamic analysis and characteristics diagnosis of seasonally perturbed predator-prey systems, *Communication in Nonlinear Science and Numerical Simulation* 22, 407-415 (2015).

L. Dai, K. Huang, T. Huang, and L. Sun, Nonlinear behavior characterization of a 3-layer laminated composite cantilever beam system, *Nonlinear Engineering.* 2, 57–69 (2014).

L. Dai, and L. Han, Analysing periodicity, nonlinearity and transitional characteristics of nonlinear dynamic systems with periodicity ratio (PR), *Communication in Nonlinear Science and Numerical Simulation,* 16, 4731- 4744 (2011).

L. Dai and L. Han, Characterizing nonlinear dynamic systems with periodicity ratio and statistic hypothesis, IMECE2011-62109, proceedings of 2011 ASME International Mechanical Engineering Congress & Exposition (IMECE), 7, 519-526 (2011).

L. Dai and G. Wang, Implementation of periodicity ratio in analyzing nonlinear dynamic systems: A comparison with Lyapunov exponent, *J. Comput. Nonlinear Dynam.* 3, 011006 (2008).

H. J. Naussbaumer, Fast Fourier Transform and Convolution Algorithms. *Springer*, (1982).

M. Henon, A two-dimensional mapping with a strange attractor, *Communications in Mathematical Physics*, 50, 69-77 (1976).

APPENDIX A

Derivation of the equations (3.1) and (3.2):

The equations governing three-dimensional response are derived by applying Hamilton's principle

$$\delta\left[\int_{T_1}^{T_2}(\amalg_T - \amalg_S + \amalg_W)dT\right] = 0 \tag{1}$$

In which, $\amalg_T$, $\amalg_S$, and $\amalg_W$ denote the cable kinetic energy, cable strain energy and the work done by gravity respectively.

The flexible cable is assumed to undergo uniform axial extensions described by the Lagrangian strain of its centerline. The finite strain description leads to the nonlinear strain-displacement relationship:

$$\varepsilon = \frac{P}{EA} + U_{1,S} - KU_2 + \frac{1}{2}\left[(U_{1,S} - KU_2)^2 + (U_{2,S} + KU_1)^2 + U_{3,S}^2\right] \tag{2}$$

in which ε is the Lagrangian strain of the cable in the final configuration, K and $P$are the cable curvature and tension in the equilibrium configuration. The strain energy of the cable in the final configuration is:

$$\amalg_S = \amalg_S^i + \int_0^L \left[P\varepsilon_d + \frac{1}{2}EA\varepsilon_d^2\right] dS \tag{3}$$

Where $\varepsilon_d = U_{1,S} - KU_2 + \frac{1}{2}\left[(U_{1,S} - KU_2)^2 + (U_{2,S} + KU_1)^2 + U_{3,S}^2\right]$

The kinetic energy of the cable is

$$\amalg_T = \int_0^L \frac{1}{2}\rho\left[(U_{1,T})^2 + (U_{2,T})^2 + (U_{3,T})^2\right]dS \tag{4}$$

The work done by gravity is:

$$\amalg_W = \amalg_w^i + \int_0^L -\rho g[U_1 \sin\theta + U_2 \cos\theta]dS \tag{5}$$

Substituting $\amalg_T$, $\amalg_S$, and $\amalg_W$ into the Hamilton's principle and integrating by parts, the following nonlinear equations can be obtained:

Tangential component U_1:

$$\left[(P + EA\varepsilon_d)(1 + U_{1,S} - KU_2)\right] - \left[(P + EA\varepsilon_d)K\left(U_{2,S} + KU_1\right)\right] - \rho g \sin\theta = \rho U_{1,TT} \tag{6}$$

Normal component U_2:

$$\left[(P + EA\varepsilon_d)\left(U_{2,S} + KU_1\right) + \left[(P + EA\varepsilon_d)K(1 + U_{1,S} - KU_2)\right]\right] - \rho g \cos\theta = \rho U_{2,TT} \tag{7}$$

Binormal component U_3:

$$\left[(P + EA\varepsilon_d)\left(U_{3,S}\right) = \rho U_{3,TT}\right] \tag{8}$$

The boundary conditions:

$$U_1(0,T) = F\cos\Omega T,\ U_1(L,T) = 0$$

$$U_i(0,T) = U_i(L,T) = 0, i = 2,3 \tag{9}$$

The solution for the equilibrium tension can be lead to:

$$P = \sqrt{P_0^2 + [\rho g(S - L/2)]^2}\ ,$$

$$K = \frac{\rho g P_0}{P_0^2 + [\rho g(S - L/2)]^2} \tag{10}$$

Where P_0 is the equilibrium cable tension at the mid-span (S=L/2).

In most applications, the cable supports substantial static tension and the resulting equilibrium curvature is quite small. Under such conditions, the parabolic approximation to the catenary is used which corresponds to the second-order Taylor series expansions of the equations about the mid-span:

$$P = P_0, K = \frac{\rho g}{P_0} \tag{11}$$

Defining the non-dimensional curvature $k = KL = \rho gL/P_0$ as a small parameter and is used to order the terms in the nonlinear equations of motion to obtain an asymptotic model for small curvature, neglecting the terms of order $k^2$and higher provides:

$$v_t^2 \left\{u_{1,s} - ku_2 + \frac{1}{2}\left[u_{2,s}^2 + u_{3,s}^2\right]\right\} = u_{1,tt} \tag{12}$$

$$\left(\left\{v_t^2 + v_l^2\left[u_{1,s} - ku_2 + \frac{1}{2}\left[u_{2,s}^2 + u_{3,s}^2\right]\right]\right\}u_{2,s}\right) + kv_t^2\left(u_{1,s} - ku_2\right) = u_{2,tt} \tag{13}$$

$$\left(\left\{v_t^2 + v_l^2\left[u_{1,s} - ku_2 + \frac{1}{2}\left[u_{2,s}^2 + u_{3,s}^2\right]\right]\right\}u_{3,s}\right) = u_{3,tt} \tag{14}$$

The following non-dimensional quantities have been used:

$$\mathrm{s} = \frac{S}{L}, t = \frac{T}{\sqrt{L/g}}, k = \frac{\rho gL}{P_0}, v_t^2 = \frac{P_0}{\rho gL} = \frac{1}{k}, v_t^2 = \frac{EA}{\rho gL}, u_i = \frac{U_i}{L}, i = 1,2,3, \tag{15}$$

The acceleration term in equation (12) is neglected under the assumption that the cable stretch in a quasi-static manner. By integration of equation (12) provides

$$u_{1,s} - ku_2 + \frac{1}{2}\left[u_{2,s}^2 + u_{3,s}^2\right] = g(t) \tag{16}$$

In which g(t) is an arbitrary function of time. Integrating again and using the boundary conditions in (9), it can be obtained:

$$u_1(s,t) = f\cos\omega t + g(t)s + \int_0^s \left[ku_2(\delta,t) - \frac{1}{2}\left\{\left[u_{2,\mu}(\delta,t)\right]^2 + \left[u_{3,\mu}(\delta,t)\right]^2\right\}\right]d\delta \tag{17}$$

Where

$$g(t) = -f\cos\omega t + \int_0^1 \left[-ku_2(\delta,t) + \frac{1}{2}\left\{\left[u_{2,\mu}(\delta,t)\right]^2 + \left[u_{3,\mu}(\delta,t)\right]^2\right\}\right]d\delta \tag{18}$$

Where $f = \frac{F}{L}, \omega = \Omega\sqrt{\frac{L}{g}}$

Taking two transverse displacement components and applying Galerkin's method using the separable solutions:

$$u_3(s,t) = x(t)\theta_{3j}(s) \tag{26}$$

$$u_2(s,t) = y(t)\theta_{2j}(s) \tag{27}$$

$\theta_{3j}(s)$ and $\theta_{2j}(s)$ are the jth out-of-plane and ith in-plane vibration mode shapes.

By applying the equation (26) and (27) and introduce the small parameter ε ,the two-degree-of-freedom model can be obtained as follows:

$$\ddot{x} + 2\varepsilon^2 c_x \dot{x} + (\omega_x^2 + 2\varepsilon^2 f_1 \cos\Omega t)x + \varepsilon^2\beta_3 xy^2 + \varepsilon^2\beta_4 x^3 - \varepsilon\alpha_2 y^2 - \varepsilon\alpha_3 x^2 = \varepsilon^2 F_1 \cos\Omega t \tag{28}$$

$$\ddot{y} + 2\varepsilon^2 c_y \dot{y} + \left(\omega_y^2 + 2\varepsilon^2 f_2 \cos\Omega t\right)y + \varepsilon^2\beta_1 y^3 + \varepsilon^2\beta_2 x^2 y - \varepsilon\alpha_1 xy = 0 \tag{29}$$

Where $\omega_x = i\pi v_t, i = 2,4,6 \ldots\ (anti-symmetric)$

$$\tan\frac{\omega_x}{2v_t} - \frac{1}{2}\left[\frac{\omega_x}{v_t} - \frac{\left({}^{\omega_1}/_{v_t}\right)^2}{\lambda^2}\right] = 0, i = 1,3,5 \ldots (symmetric)$$

$\omega_y = i\pi v_t, i = 1,2,3 \ldots$

where λ is the parameter with respect to the cable derived in [1]

$$\lambda^2 = \frac{v_l^2}{(v_t^2)^3}$$

where $v_t^2 = \frac{P_0}{\rho g L} = \frac{1}{k},\ v_l^2 = \frac{EA}{\rho g L}$

ρ indicates the density of the cable, g is the gravity, P_0 is the equilibrium cable tension at mid-span, L is the length of the cable, EA is the section stiffness of the elastic cable cross-section.

$$\alpha_1 = \frac{v_l^2}{(v_t^2)^2}\omega_2^2\theta_1, \alpha_2 = \frac{1}{2}\alpha_1, \alpha_3 = \frac{3v_l^2}{2(v_t^2)^2}\gamma^2\theta_1,$$

$$\beta_1 = \frac{v_l^2}{2(v_t^2)^2}\omega_2^4, \beta_2 = \beta_3 = \frac{v_l^2}{2(v_t^2)^2}\gamma^2\omega_2^2, \beta_4 = \frac{v_l^2}{2(v_t^2)^2}\gamma^4,$$

$$f_1 = -\frac{Fv_l^2}{2Lv_t^2}\gamma^2,\ f_2 = -\frac{Fv_l^2}{2Lv_t^2}\omega_y^2, F_1 = -\frac{Fv_l^2}{Lv_t^2}\theta_1,$$

where $\gamma^2 = \omega_x^2 - \frac{v_l^2}{(v_t^2)^2}\theta_2^2$,

$$\theta_1 = \int_0^1 \theta_{1i}(\eta)d\eta = \begin{cases} 0 & antisymmetric \\ Q\left[1 + \dfrac{2v_t\left[\cos\left(\omega_x/v_t\right) - 1\right]}{\omega_x \sin\left(\omega_x/v_t\right)}\right] & symmetric \end{cases}$$

APPENDIX B

$$\gamma_1 = -2\beta_3 - \frac{4\alpha_1\alpha_2}{3\omega^2} + \frac{4\alpha_2\alpha_3}{\omega^2}$$

$$\gamma_2 = -3\beta_4 + \frac{10\alpha_3^2}{3\omega^2}$$

$$\gamma_3 = \frac{2\alpha_1\alpha_2}{\omega^2} - \frac{2\alpha_2\alpha_3}{3\omega^2} - \beta_3$$

$$\gamma_4 = -3\beta_1 + \frac{5\alpha_1\alpha_2}{3\omega^2}$$

$$\gamma_5 = -\beta_2 + \frac{\alpha_1^2}{\omega^2} - \frac{\alpha_1\alpha_3}{3\omega^2}$$

$$\gamma_6 = -2\beta_2 + \frac{2\alpha_1^2}{3\omega^2} + \frac{2\alpha_1\alpha_3}{\omega^2}$$

APPENDIX C

$$\tau_1 = \gamma_2^2$$

$$\tau_2 = 2\gamma_2(\gamma_1 + \gamma_3)b^2 - 2\gamma_2\sigma_1$$

$$\tau_3 = [(\gamma_1 + \gamma_3)b^2 - \sigma_1]^2 + 4\omega^2 c_x^2 - f_1^2$$

$$\tau_4 = \gamma_4^2$$

$$\tau_5 = 2\gamma_4(\gamma_5 + \gamma_6)a^2 - 2\gamma_4\sigma_1$$

$$\tau_6 = [(\gamma_5 + \gamma_6)a^2 - \sigma_2]^2 + 4\omega^2 c_y^2 - f_2^2$$

APPENDIX D

Main MATLAB code for Lyapunov exponent

```
global k b v

yinit = [1,1,1];

orthmatrix = [1 0 0; 0 1 0;0 0 1];

y = zeros (12,1);

y(1:3) = yinit;

y(4:12) = orthmatrix;

tstart = 0;

tstep = 1;

wholetimes =4*1e3;

steps =1;

iteratetimes = wholetimes/steps;

mod = zeros(3,1);

lp = zeros(3,1);

Lyapunov1 = zeros(iteratetimes,1);

Lyapunov2 = zeros(iteratetimes,1);

Lyapunov3 = zeros(iteratetimes,1);

figure;

hold on;

for i=1:iteratetimes

    tspan =tstart:tstep:(tstart + tstep*steps);

    [T,Y] = ode45('Duffing_lynew', tspan, y);

    y = Y(size(Y,1),:)

    tstart = tstart + tstep*steps;
```

```
    y0 = [y(4) y(7) y(10);  y(5) y(8) y(11); y(6) y(9) y(12)];
    y0 = ThreeGS(y0);
    mod(1) = sqrt(y0(:,1)'*y0(:,1));
    mod(2) = sqrt(y0(:,2)'*y0(:,2));
    mod(3) = sqrt(y0(:,3)'*y0(:,3));
    y0(:,1) = y0(:,1)/mod(1);
    y0(:,2) = y0(:,2)/mod(2);
    y0(:,3) = y0(:,3)/mod(3);
    lp = lp+log(abs(mod));
    Lyapunov1(i) = lp(1)/(tstart);
    Lyapunov2(i) = lp(2)/(tstart);
    Lyapunov3(i) = lp(3)/(tstart);
y(4:12) = y0;
    hold on;
end
figure;
i = 1:iteratetimes;
 plot(i,Lyapunov1(i),i,Lyapunov2(i),i,Lyapunov3(i),'linewidth',2)
```

APPENDIX E

Main MATLAB code for the periodicity ratio

```
clc;
 tic
  [x,y,t]=RKduffing2(x0,y0,k,b,v,hh,n);
 n2=floor((n-n1)/(aa));xx=zeros(1,n2); xx1=zeros(1,n2);
  for i=1:n2
     xx(i)=x(n1+round((i-1)*(aa)));
     xx1(i)=y(n1+round((i-1)*(aa)));
  end
  z=zeros(n2,n2);
for i=1:n2
    for j=i:n2
    z(i,j)=sqrt((xx(i)-xx(j))^2+(xx1(i)-xx1(j))^2);
    if z(i,j)<0.0005          %value for calculation of overlapping points,(10^(-6))~(10^(-4))respond
to 1~10 of phase diagram
       z(i,j)=1;
    else
       z(i,j)=0;
    end
    end
end
for ii=1:n2-2
    zz=z(ii,ii+1:n2);
    zza=find(zz==1);
```

```
    if length(zza)>=1
        for t=1:length(zza)
            z(zza(t)+ii,zza(t)+ii+1:n2)=0;
    end
    end
end
for k1=3:n2
a=z(1:k1-1,k1);
b=find(a==1);
if length(b)>1
        z(b(1)+1:k1-1,k1)=0;
end
end
e=zeros(1,n2);
for t=1:n2
c=z(t,:);
d=find(c==1);
if length(d)>1
    e(t)=length(d);
else
    e(t)=0;
end
end
sum=0;
for t=1:n2
    sum=sum+e(t);
```

```
end
prx=sum/n2                    %need to find it in workspace
toc
```